UPR^{ER}–immunity axis acts as physiological food evaluation system that promotes aversion behavior in sensing low-quality food

Pengfei Liu, Xinyi Liu, Bin Qi[1,2]

Southwest United Graduate School,Yunnan Key Laboratory of Cell Metabolism and Diseases, State Key Laboratory of Conservation and Utilization of Bio-resources in Yunnan, Center for Life Sciences, School of Life Sciences, Yunnan University, Kunming, China

Footnotes: 1 Corresponding Author (Bin Qi, Email: qb@ynu.edu.cn)

Footnotes: 2 Lead Contact (Bin Qi, Email: qb@ynu.edu.cn)

Abstract

To survive in challenging environments, animals must develop a system to assess food quality and adjust their feeding behavior accordingly. However, the mechanisms that regulate this chronic physiological food evaluation system, which monitors specific nutrients from ingested food and influences food-response behavior, are still not fully understood. Here, we established a low-quality food evaluation assay system and found that heat-killed *E. coli* (HK-*E. coli),* a low sugar food, triggers cellular UPR^{ER} and immune response. This encourages animals to avoid low-quality food. The physiological system

for evaluating low-quality food depends on the UPR^{ER} (IRE-1/XBP-1) - Innate immunity (PMK-1/p38 MAPK) axis, particularly its neuronal function, which subsequently regulates feeding behaviors. Moreover, animals can adapt to a low-quality food environment through sugar supplementation, which inhibits the UPR^{ER} -PMK-1 regulated stress response by increasing vitamin C biosynthesis. This study reveals the role of the cellular stress response pathway as physiological food evaluation system for assessing nutritional deficiencies in food, thereby enhancing survival in natural environments.

Keywords: aversion behavior; UPR^{ER}; immune response; XBP-1; PMK-1; Food quality evaluation; Food sensing; *C. elegans*;

Introduction

Food is essential for the survival, growth and fitness of all animals. To adapt to fluctuating environments with a wide range of food sources, animals have developed a food evaluation system. This system enables them to identify nutrient-rich food and avoids low-quality or toxic food, thereby maximizing their survival prospects [1, 2, 3]. Various sensory neuron evaluation systems in animals has evolved to evaluate food quality through vision [4, 5], olfactory [3, 6, 7, 8, 9, 10, 11, 12] and gustatory senses [13, 14, 15]. Besides these sensory systems that facilitate quick feeding decisions, animals may also initiate cellular stress response programs to detect nutrition/toxin and trigger food response behaviors [16, 17]. This could be one of physiological food quality evaluation systems that monitor the nutritional status of consumed food. However, the signaling events in cellular stress responses involved in evaluating of specific nutrients and the mechanisms that connect these signaling activities to food behaviors are largely unexplored. More specifically, while cellular stress response through UPR^{ER} [18]

and PMK-1/p38 MAPK [19] dependent immunity in response to pathogens have been extensively studied, the functions of these cellular stress response in sensing and evaluating specific nutrients from food remain unclear.

Vitamin C is an essential micronutrient that cannot be synthesized by humans due to the loss of a key enzyme in the biosynthetic pathway [20]. Animals obtain vitamin C from their diet and possibly also from gut microbes [21]. Vitamin C is an important physiological antioxidant and a cofactor for a family of biosynthetic and gene regulatory monooxygenase and dioxygenase enzymes. It is also required for the biosynthesis of collagen, L-carnitine, and certain neurotransmitters [22, 23]. Vitamin C has been associated with various human diseases including scurvy, immune defect and cardiovascular disease [20]. Therefore, in animals, having robust food evaluation systems to detect vitamin C levels could significantly impact their survival in the wild. However, the potential involvement of the cellular stress response pathway in this food evaluation system for sensing and assessing vitamin C remains largely unexplored.

In this study, using the low-quality food evaluation assay system we established [24], we elucidated the mechanism by which the cellular stress response pathway operates as a physiological food evaluation system. This pathway assesses the deficiency of D-glucose in food and the subsequent vitamin C content in animals through the unfolded protein response (UPR^{ER}) - innate immunity (PMK-1/p38 MAPK) axis. This mechanism promotes animals to leave low-quality food and is critical for their survival in nature environments.

Results

78

79 **Low-quality food induces stress response in animals**

80 Our previous studies have shown that Heat-killed *E. coli* (HK-*E. coli*), which
81 lacks certain molecules, is considered a low-quality food that is unable to
82 support animal growth [24, 25]. Moreover, through metabolic-seq analysis, we
83 identified significant changes in a large numbers of derivatives (Figure 1-
84 figure supplement 1A, Table S1)，including lipids and their derivatives (Figure
85 1-figure supplement 1B, Table S1)，amino acid and their metabolites (Figure
86 1-figure supplement 1C, Table S1), as well as coenzymes and vitamins
87 (Figure 1-figure supplement 1D, Table S1). Interestingly, we observed a
88 significant decrease in carboxylic acids and their derivatives (Figure 1-figure
89 supplement 1E, Table S1) in *E. coli* after being heat-killed (Figure 1-figure
90 supplement 1F, Table S1). This suggests that HK-*E. coli* is nutritionally
91 deficient for *C. elegans* when compared to normal *E. coli* food.

92

93 Next, we conducted two behavior assays to facilitate the analysis of the food
94 evaluation process in animals by seeding L1 animals in assay plates (Figure
95 1A and 1B). In the avoidance assay, wild-type animals avoided the HK-*E. coli*
96 OP50 (HK-OP50) food (Figure 1A). Interestingly, in the food choice assay,
97 animals initially showed no preference between the two types of food (1-2h),
98 but eventually exhibited a preference for high-quality food (Live *E. coli*) up until
99 the 17h mark (Figure 1B, Figure 1-figure supplement 1G). This suggests that
100 worms depart from the HK-*E. coli* after recognizing it as low-quality food source
101 through ingestion.

102

103 In order to investigate the pathways in animals that respond to HK-*E. coli*, we
104 performed transcriptomics analysis on worms that were cultured with both HK-
105 *E. coli* and Live *E. coli*. Gene-expression profiling revealed that stress response

genes, including those related to biotic stimulus, immune response and response to stress, are up-regulated in animals fed with HK-*E. coli* OP50 (HK-OP50) (Figure 1C, Table S2). Among these up-regulated genes, we identified 11 out of 62 of UPR^{ER} target genes (Figure 1D, Figure 1-figure supplement 1H and Table S2). Additionally, about 50%-80% of up-regulated genes overlap with genes responding pathogenic bacteria [26, 27] (Figure 1E, Table S2). Consistent with the results of the RNA sequencing (RNA-seq) analysis, the UPR^{ER} reporter (*Phsp-4::GFP*)[28] and immunity reporter (*Pirg-5::GFP*)[29] were strongly induced in intestine (Figure 1F-G) and neurons (Figure 1-figure supplement 2A) by feeding unfavorable food (HK-*E. coli* OP50), suggesting that UPR^{ER} and immune pathways may respond to low-quality food (HK-*E. coli* OP50). As intestinal fluorescence (*Phsp-4::GFP or Pirg-5::GFP)* is easy observation and scoring, the further analyses were done in the intestine.

Moreover, UPR^{Mt} reporter (*Phsp-6::GFP*) [30] was weakly induced under HK-*E. coli* feeding condition (Figure 1-figure supplement 2B), and starved worm did not induce UPR^{ER} and immunity (Figure 1-figure supplement 2C-D).

Together, these findings suggest that low-quality food (HK-*E. coli* OP50) triggers a stress response pathway in animals, including UPR^{ER} and innate immune pathway. This implies that animals may assess the quality of food through UPR^{ER} and innate immune pathway.

Animals evaluate food quality through UPR^{ER}-immune-dependent physiological food quality evaluation system

To determine whether the UPR^{ER} and innate immune pathways play a role in evaluating low-quality food, we first examined whether the activation of the

134 UPR^{ER} by HK-*E. coli* was dependent on the known signaling components of the
135 UPR^{ER} branches, including IRE/XBP-1, PERK/ATF-4 and ATF-6 [31, 32]. We
136 observed no difference in *Phsp-4::GFP* induction with *atf-4* (Figure 2-figure
137 supplement 1A) or *atf-6* (Figure 2-figure supplement 1B) RNAi-mediated
138 knockdown in animals fed with HK-*E. coli*. However, knockdown of *ire-1/xbp-1*
139 or mutation of *xbp-1* reduced GFP fluorescence (Figure 2A, 2B). Among the 11
140 differentially expressed UPR^{ER} target genes in animals fed with HK-*E. coli* from
141 RNA-seq (Figure 1D), 64% of the genes are IRE-mediated genes (Figure 1-
142 figure supplement 1H, Table S2). The mRNA level of IRE-1-mediated splicing
143 of *xbp-1*[28] is also induced in animals fed with HK-*E. coli* OP50 (Figure 2-figure
144 supplement 1C). However, UPR^{ER} is not affect in animals feeding live-*E. coli* by
145 RNAi of *ire-1, xpb-1, atf-4* and *atf-6* (Figure 2-figure supplement 1D). These
146 data suggest that activation of the UPR^{ER} by low-quality food (HK-*E. coli*)
147 depends on the IRE-1/XBP-1.
148
149 To further analyze whether XBP-1-dependent UPR^{ER} activation is critical for
150 animals to leave low-quality food, we tested food avoidance behavior using *xbp-*
151 *1* mutant. The results show that *xbp-1* mutants had a significantly decreased
152 likelihood of leaving of HK-*E. coli*, which was rescued by expressing *xbp-1* in
153 neuron rather than intestine (Figure 2C). This indicates that XBP-1-dependent
154 UPR^{ER} activation in neuron is critical for animals to specific evaluate low-quality
155 food (HK-*E. coli*).
156
157 We then investigated which innate immune pathway is involved in evaluating
158 low-quality food. First, we analyzed HK-*E. coli* induced genes from RNA-seq.
159 Among these up-regulated genes, 82 out of 409 of PMK-1-dependent genes [33]
160 were identified (Figure 2-figure supplement 1E, Table S2). Second, we
161 confirmed the induction of several well-known PMK-1 target genes in RNA-seq

162 data[34] (Figure 2-figure supplement 1F) and reporter analysis (Figure 2-figure
163 supplement 1G-H). Moreover, the induction of *Pirg-5::GFP* was abolished in
164 *pmk-1* knockdown animals fed with HK-*E. coli* (Figure 2D). Third, we found that
165 the phosphorylated PMK-1 (p-PMK-1) level was prominently increased in wild-
166 type N2 animals fed HK-*E. coli* compared to feeding *E. coli* OP50 (Figure 2E).
167 Finally, *pmk-1* mutants had a decreased likelihood of leaving of HK-*E. coli*,
168 which was rescued by expressing *pmk-1* in neurons rather than intestine
169 (Figure 2F). Moreover, *Pirg-5::GFP* is not affect in animals feeding live-*E. coli*
170 by RNAi of *pmk-1* (Figure 2-figure supplement 1I).These data suggest that
171 PMK-1 regulated immune pathway evaluates low-quality food, especially the
172 neuronal PMK-1 has a critical function for food quality response.
173
174 **XBP-1 and PMK-1 are in the same pathway for evaluating food quality**
175
176 Next, we explored the connection between UPR^{ER} (IRE-1/XBP-1) and innate
177 immunity (PMK-1 p38 MAPK) in food quality evaluation. We found that *Pirg-*
178 *5::GFP* induction (Figure 2-figure supplement 1I, 2A) and PMK-1 activation
179 (Figure 2E) were decreased in animals with *xbp-1* mutation or knockdown when
180 fed with HK-*E. coli*, suggesting that XBP-1 could regulate PMK-1 under this
181 condition. Additionally, *Phsp-4::GFP* induction under HK-*E. coli was* not
182 affected in animals with *pmk-1* RNAi (Figure 2-figure supplement 1D, 2B),
183 indicating that XBP-1-dependent UPR^{ER} activation is not regulated by PMK-1.
184 Finally, we constructed a double mutant of *xbp-1* and *pmk-1* and found that the
185 food avoidance phenotype of the double mutant was similar to the *pmk-1*
186 mutant (Figure 2G), indicating that PMK-1 is downstream of XBP-1 in
187 responding to low-quality food.
188
189 We then asked whether UPR^{ER} (IRE-1/XBP-1) - Innate immunity (PMK-1/p38

190 MAPK) axis is specific to evaluate low-quality food (HK-*E. coli*). We performed
191 behavior assay in N2, *pmk-1* and *xbp-1* mutant animals by feeding normal *E.*
192 *coli* food, inedible food (*Saprophytic staphylococci)* [35] and pathogenic food
193 (*Pseudomonas aeruginosa-PA14)* [18]. We found that N2, *pmk-1*, and *xbp-1*
194 mutant worms did not exhibit avoidance behavior when presented with normal
195 food (OP50). However, both N2 and *xbp-1* mutant worms were able to escape
196 from inedible food (N2 was predominantly found on the border areas of the
197 bacterial lawn and *xbp-1* mutant worms on border and in), *Saprophytic*
198 *staphylococci*, whereas *pmk-1* mutant worms did not exhibit this avoidance
199 behavior. Notably, N2 and *xbp-1* mutant worms exhibited even more
200 pronounced avoidance behavior when exposed to *Pseudomonas aeruginosa*,
201 whereas *pmk-1* mutant worms were more susceptible to infection by this
202 pathogen (Figure 2-figure supplement 2C). These findings suggest that the
203 UPR-Immunity pathway plays a crucial role in helping animals avoid low-
204 quality food (HK-*E. coli*) by triggering an avoidance response. In contrast, the
205 Innate immunity pathway, which is mediated by PMK-1/p38 MAPK, appears to
206 play a key role in evaluating unfavorable food sources, such as HK-*E. coli*,
207 *Saprophytic staphylococci*, and *Pseudomonas aeruginosa*, and helping
208 animals avoid these environments.
209
210
211 **Sugar deficiency in HK-*E. coli* food induces stress response and**
212 **avoidance behavior in animals**
213
214 We then investigated which nutrients/metabolites are sensed by animals
215 through the XBP-1-PMK-1 axis for food quality evaluation. First, we
216 hypothesized that the nutrition status is improved in *E. coli* mutant (HK-
217 treatment), which could inhibit UPR^{ER} and immune response in animals. We

218 established a system for screening the *E. coli* mutant Keio library (Figure 3-
219 figure supplement 1A), and identified 20 *E. coli* mutants that did not induce
220 *Phsp-4::GFP* through the UPR^{ER} reporter (*Phsp-4::GFP*) after three rounds of
221 screening (Table S3). From these 20 *E. coli* mutants, we identified 9 *E. coli*
222 mutants that did not induce *Pirg-5::GFP* through the immunity reporter (*Pirg-*
223 *5::GFP*) screening (Figure 3-figure supplement 1B-C, Table S3). Animals fed
224 HK-*yfbR*, which catalyzes carbohydrate derivative metabolic process[36], had a
225 decreased ability to leave food (Figure 3A, Table S3), indicating that HK-*yfbR*
226 may be a higher quality food for animals compared to HK-K12.
227
228 Secondly, we performed a metabolomics analysis of different quality food (HK-
229 K12, HK-*yfbR* and Live-K12). We found that the level of 13 metabolites were
230 similar between HK-*yfbR* and Live-K12, but significantly changed in HK-K12
231 (Figure 3B, Figure 3-figure supplement 2A, and Table S1). We also found that
232 genes involved in glycolysis/gluconeogenesis were up-regulated in animals fed
233 with HK-*E. coli* (Figure 3-figure supplement 2B), suggesting that
234 glycolysis/gluconeogenesis metabolism is disordered in animals fed with HK-*E.*
235 *coli,* which may result from changes in sugar/carbohydrate intake. The
236 carbohydrates (D-trehalose, lactose, and D-(+)-sucrose) were also decreased
237 in HK-*E. coli* (Figure 3B), suggesting that carbohydrate deficiency may induce
238 stress response and avoidance behavior in animals feeding HK-*E. coli*.
239
240 Thirdly, to determine which carbohydrate inhibits stress response in animals,
241 we supplemented each metabolite to HK-*E. coli* and found that only Lactose,
242 and D-(+)-sucrose inhibited HK-*E. coli* induced UPR^{ER} (Figure 3C and 3D,
243 Figure 3-figure supplement 2C). Moreover, we found from our metabolomic
244 data that the sugar level, including lactose, and D-(+)-sucrose, and D-(+)-
245 glucose, was also decreased in HK-*E. coli* (Figure 3B, Table S1). Since lactose

246 and D-(+)-sucrose are hydrolyzed to produce glucose[37, 38], we wondered
247 whether glucose also inhibits the stress response in animals. We found that D-
248 (+)-glucose supplementation also inhibited HK-*E. coli* induced UPR^{ER} (Figure
249 3E), immune response (Figure 3F, 3G and Figure 3-figure supplement 2D) and
250 avoidance (Figure 3H). Moreover, sugar supplementation did not affect UPR^{ER}
251 and immunity in normal food (OP50) or starved condition (NGM) (Figure 3-
252 figure supplement 2E-F). While sugar effectively inhibits the HK-*E. coli*-induced
253 UPR^{ER} and immune response, it does not fully suppress it to the extent
254 observed with live-*E. coli* (Figure 3C-F). This implies that additional nutrients
255 present in live-*E. coli* might also contribute to the inhibition of UPR^{ER} and
256 immune response.
257
258 Previous studies have shown that heat-killed *E. coli* (HK-*E. coli*) is a low-quality
259 food source that cannot support the growth of *C. elegans* larvae[24, 25], whereas
260 supplementation with vitamin B2 (VB2) can restore animal growth[24]. Here, we
261 found that sugar deficiency in HK-*E. coli* induces the UPR^{ER}-immune response
262 and avoidance behavior in *C. elegans*. Given this, we investigated whether
263 sugar supplementation could promote animal growth when fed HK-*E. coli.* To
264 our surprise, supplementing HK-*E. coli* with carbohydrates (D-Glc, D-GlcA) did
265 not support animal development (Figure 3-figure supplement 2G), suggesting
266 that carbohydrates are not essential for supporting animal growth on this food
267 source. However, we did find that carbohydrates are critical for inhibiting the
268 UPR^{ER}-immune response induced by sugar deficiency in HK-*E. coli.*
269
270 Together, these findings suggest that HK-*E. coli* induces a stress response and
271 avoidance behavior in animals, which can be inhibited by D-(+)-glucose
272 supplementation. This implies that animals may evaluate the sugar deficiency
273 from HK-*E. coli* through the activation of UPR^{ER} and immune responses.

274

275

276 **Animals could overcome a low-quality food environment by sugar**
277 **supplementation through vitamin C biosynthesis**

278

279 We discovered that D-(+)-glucose supplementation inhibited HK-*E. coli* induced
280 UPR^{ER} (Figure 3E), immune response (Figure 3F, 3G and Figure 3-figure
281 supplement 2D) and avoidance (Figure 3H). Simultaneously, vitamin C (VC),
282 which is synthesized by glucuronate pathway using D-glucose [39, 40] (Figure 4A),
283 was found to contribute to neuroprotective[41, 42], immune defense[43, 44], and
284 inhibits inflammatory and ER stress[45, 46]. This led us to question whether the
285 vitamin C biosynthesis pathway is involved in evaluating low-quality food by
286 using D-glucose.

287

288 Firstly, we observed an increase in the vitamin C level in *C. elegans* when fed
289 with HK-*yfbR* (Figure 4B), a high carbohydrate food compared to HK-*E. coli*
290 (Figure 3B and Figure 1-figure supplement 1E). However, the VC level in
291 bacteria is the same (Figure 4-figure supplement 1A). The VC level also
292 increased when D-glucose (Figure 4-figure supplement 1B) or D-glucuronate
293 (D-GlcA) was added to HK-*E. coli* (Figure 4C), which was abolished by
294 knocking down VC biosynthesis genes (Figure 4C and Figure 4-figure
295 supplement 1B). This suggests that addition of sugar supplementation
296 promotes VC synthesis in animals fed with HK-*E. coli.*

297

298 Secondly, we hypothesized that animals could overcome a low-quality food
299 (HK-*E. coli*) environment by inhibiting the stress response through increasing
300 vitamin C biosynthesis. We found that VC or D-glucuronate (D-GlcA)
301 supplementation inhibits HK-*E. coli* induced UPR^{ER} (Figure 4D), immune

302 response including *irg-5/sysm-1* reporter expression (Figure 4E and Figure 4-
303 figure supplement 1C) and p-PMK-1 (Figure 4F and 4G), as well as food
304 avoidance (Figure 4H).
305
306 Finally, we asked whether inhibition of stress response and avoidance by sugar
307 supplementation depends on the vitamin C biosynthesis pathway. We found
308 that suppression of HK-*E. coli* induced UPR^{ER} (Figure 4I), immune response
309 (Figure 4J and Figure 4-figure supplement 1D) and food avoidance (Figure 4K)
310 by D-GlcA/sugar supplementation was abolished in animals with RNAi of VC
311 biosynthesis genes. Food selection behavior assays showed that D-GlcA/sugar
312 supplementation increased the preference for heat-killed bacteria, which was
313 also suppressed by knocking down VC biosynthesis genes (Figure 4-figure
314 supplement 1E). However, VC supplementation still suppressed the UPR^{ER}
315 (Figure 4I), immune response (Figure 4J and Figure 4-figure supplement 1D)
316 and food avoidance (Figure 4K), and increased the food preference (Figure 4-
317 figure supplement 1E) in animals with or without RNAi of VC biosynthesis genes.
318 This suggests that VC, as the final metabolite synthesized from D-glucose, is
319 critical for evaluating low-quality food response in animals.
320 Together, these data indicate that the vitamin C biosynthesis pathway is critical
321 for evaluating whether food is of higher quality and can be eaten by animals. It
322 also suggests that animals could improve their VC levels to adapt to bad food
323 environment.
324
325 **Animals evaluate sugar and vitamin C through neuronal XBP-1 and PMK-**
326 **1**
327 As D-GlcA/sugar and VC supplementation suppressed HK-*E. coli* induced
328 UPR^{ER}, immune response and food avoidance behavior, we investigated
329 whether animals evaluate sugar and VC through XBP and PMK-1 dependent

330 pathways. We performed a food selection behavior assay by adding D-Glc, D-
331 GlcA or VC to the NGM, *E. coli* and HK-*E. coli* (Figure 5A). The food selection
332 behavior assays revealed that supplementation with D-Glc, D-GlcA, or VC
333 inhibits the animals' choice of sugar or VC on *E. coli*-OP50 feeding conditions
334 (Figure 5-figure supplement 1A). This suggests that supplementation with D-
335 Glc, D-GlcA, or VC may alter the metabolites of live bacteria, leading to
336 avoidance by the animals. There was no preference observed on NGM plate
337 (no food condition) supplementation with D-Glc and VC (Figure 5-figure
338 supplement 1B), indicating that the intake of sugar or VC alone does not
339 influence animal preference. However, alone D-GlcA could influence worm
340 physiology which induces preference change (Figure 5-figure supplement 1B).
341 Interestingly, D-Glc and D-GlcA (Figure 5B and 5C) or VC (Figure 5D)
342 supplementation increased the preference for heat-killed bacteria, which was
343 suppressed in *xbp-1* or *pmk-1* mutant animals. However, this preference was
344 also rescued in *xbp-1* or *pmk-1* mutant animals by expressing XBP-1 or PMK-
345 1 in neurons rather than intestine (Figure 5B-D), indicating that neuronal XBP-
346 1 and PMK-1 are critical for physiological food elevation system for monitoring
347 the level of sugar and VC under low-quality food condition.
348
349
350 **Discussion**
351 To better survive, animals must evolve a system to recognize and evaluate the
352 quality of their food. This includes the sensory neuron evaluation system for
353 immediate response and feeding decision [2], as well as physiological food
354 evaluation system for chronic response to ingested food. In our previous study,
355 we discovered that the TORC1-ELT-2 pathway, acting as master regulators in
356 intestine, evaluates vitamin B2 deficiency in low-quality food (HK-*E. coli)* and
357 regulates gut digestive activity to impact animal's food behavior [24]. To further

358 identified the mechanism by which animals evaluate low-quality food (HK-*E.*
359 *coli*), we performed metabolomics and transcriptomics analyses to identify
360 specific nutrition deficiencies in low-quality food and the cellular response
361 pathways that are involved in food evaluation pathway. This study identified a
362 physiological food evaluation mechanism by which animals recognize food
363 quality through UPR^{ER} (IRE-1/XBP-1) - Innate immunity (PMK-1/p38 MAPK)
364 regulated cellular stress response program in neurons that dictates food
365 avoidance and selection behaviors (Figure 6).
366
367 One of the cellular stress response pathways, the Unfolded Protein Response
368 (UPR^{ER}), is activated by various stresses, including infection and nutrition
369 deficiency, which disrupt the homeostasis of the endoplasmic reticulum (ER)[31].
370 The activation of UPR^{ER}, specifically in the nervous system, has been shown to
371 promote changes in feeding and foraging behavior[47]. The p38 PMK-1 pathway
372 is also crucial for regulating the expression of secreted innate immune effectors
373 and is essential for survival during infection[48]. Therefore, these two pathways
374 play a critical role in ensuring animals' survival in changing environments.
375 However, it is still unclear whether UPR^{ER} and innate immunity evaluate food
376 quality under physiological conditions. Our study provides evidence that low-
377 quality food (HK-*E. coli*) activates both UPR^{ER} and p-PMK-1, leading to animals
378 leaving the low-quality food. Previously finding have shown that inhibition of ER
379 function promotes *C. elegans* avoid to the toxic food, which employs the MLK-
380 1/MEK-1/KGB-1 pathway[49]. Notably, HK-*E. coli* induced avoidance behavior is
381 independent of the KGB-1 pathway (Figure 5-figure supplement 1C).
382 Additionally, our study reveals that neuronal UPR^{ER} and PMK-1 are essential
383 for evaluating low-quality food, suggesting that the nervous system plays a
384 critical role in assessing food quality.
385

386 Previous studies have shown that XBP1 deficiency in intestinal epithelial cells
387 leads to IRE1a hyperactivation and increased JNK phosphorylation in the
388 epithelial compartment in vivo[50]. The IRE1-XBP1 axis has been identified as a
389 critical protective branch of the Unfolded Protein Response (UPR) induced
390 secondary to an innate immune response in the presence of *P. aeruginosa* [18,
391 51]. The p38 MAPK has also been shown to directly act on the phosphorylation
392 of IRE-1 to promote the stress response[52, 53]. Interestingly, IRE-1 has been
393 found to confer cold resistance independently of XBP-1 by activating JNK-1
394 MAPK[49]. In contrast, our study reveals a new mechanism where the UPR^{ER}
395 (IRE-1/XBP-1) positively regulates Innate Immunity (PMK-1/p38 MAPK) under
396 HK-*E. coli* food conditions, establishing a novel physiological food evaluation
397 system that activates the cellular stress response program.
398
399 A previous study has shown that activating innate immunity (PMK-1 MAPK)
400 leads to a reduction in translation[54]. Our own previous research has also
401 demonstrated that PMK-1 activation causes a shutdown of food digestion in
402 animals[35], likely to reduce protein translation and cellular metabolism. To
403 investigate this further, we measured the translation level of animals fed with
404 HK-*E. coli* and found that total translation ability is significantly reduced in these
405 animals (Figure 5-figure supplement 1D). This finding suggests that activating
406 innate immunity (PMK-1 MAPK) may serve as a mechanism to slow down
407 translation progress, thereby alleviating the pressure on the unfolded protein
408 response (UPR) and preventing excessive UPR^{ER} activation.
409
410 Vitamin C (VC) is an important physiological antioxidant and a cofactor for a
411 family of biosynthetic and gene regulatory monooxygenase and dioxygenase
412 enzymes. It is also required for the biosynthesis of collagen, L-carnitine, and
413 certain neurotransmitters [22, 23]. Meanwhile, VC helps animals to protect

414 neuron[41, 42], defend excessive immune [43, 44], and inhibit inflammatory and ER
415 stress[45, 46] in order to better survive. The synthesis of vitamin C (VC) occurs
416 through the glucuronate pathway, utilizing D-glucose as a precursor [39, 40] (Figure
417 4A). This led us to investigate whether the vitamin C biosynthesis pathway is
418 involved in evaluating low-quality food by using D-glucose. In this study, we
419 found that animals feeding live *E. coli*, which should produce more VC, exhibit
420 higher glucose levels. However, our results show that animals maintain similar
421 VC levels when fed ideal food (live *E. coli*) compared to low-quality food (HK-*E.*
422 *coli*) (Figure 4B), suggesting that animals do not stimulate VC biosynthesis
423 under favorable food conditions. In contrast, when animals are fed low-quality
424 food (HK-OP50), we found that supplementing D-GlcA in HK-*E. coli* or *E. coli*-
425 *yfbR* mutation can improve VC levels and inhibit UPR^{ER}-immunity (Figure 4C).
426 These data indicate that glucose boosts the animal's ability to adapt to
427 unfavorable food environments by increasing VC levels, but not in favorable
428 food conditions.
429

430 Unlike the sensory neuron evaluation system, which permits rapid feeding
431 decisions through smell and taste, the cellular stress response as
432 physiological food evaluation system describe here requires a slow and multi-
433 step signal transduction process after the ingestion of food. The disruption of
434 cellular homeostasis by ingested of low-quality or toxic food can activate
435 stress response mechanisms that both increase the cellular ability to
436 withstand and adapt to this disruption of homeostasis and promote behavioral
437 strategies to avoid these conditions and lessen their impact on the organism.
438 These cellular stress response mechanisms include heat shock response,
439 unfolded protein response, oxidative stress response [55]. Therefore, this slow
440 physiological food evaluation system is an evolutionary adaptation

441 mechanism for detecting nutrition deficiencies in food that was not detected
442 by quick sensory nervous system.

443

444 One limitation of our study is the lack of explanation for why HK-*E. coli* activates
445 UPR^{ER} and immunity. We hypothesized that when heat-killed, HK-*E. coli* may
446 lack or contain altered levels of certain metabolites that either activate or inhibit
447 UPR^{ER} and immunity, respectively. Additionally, we speculated that *E. coli*
448 mutants killed by heat may lack metabolites that activate UPR^{ER} and immunity,
449 or conversely, have increased levels of metabolites that inhibit these pathways.
450 Fortunately, our investigation led to the discovery of the *E. coli* mutant *yfbR*,
451 which inhibits UPR^{ER} and immunity by increasing carbohydrates that aid in
452 resisting these stress pathways. Moving forward, we intend to further explore
453 the intricate relationship between HK-*E. coli* and UPR^{ER}-immunity. This will be
454 a key focus of our future research efforts.

455

456 Collectively, this study uncovers the unexpected function of UPR^{ER} (IRE-
457 1/XBP-1) - Innate immunity (PMK-1/p38 MAPK) as a physiological food
458 evaluation system for evaluating and sensing food quality in animals. It also
459 highlights the utility of the HK-*E. coli* (low-quality food) - *C. elegans* interaction
460 as a means to dissect the mechanism of food evaluation system in assessing
461 food. Most importantly, it reveals that animals are capable of altering their
462 nutrient (Vitamin C) levels through in vivo synthesis or food intake to adapt to
463 a poor food environment when better food choices are not available.

464

465 **Author Contributions**

P. L designed, performed experiments, analyzed data. X. L constructed all transgenic animals. B.Q. designed research, supervised this study, and wrote the paper with inputs from P. L.

Acknowledgments

We thank the Caenorhabditis Genetics Center (CGC) (funded by NIH P40OD010440) for strains; Dr. Zhao Shan for suggestions. This work was supported by the Ministry of Science and Technology of the People's Republic of China (2019YFA0802100, 2019YFA0803100), the National Natural Science Foundation of China (32170794), Yunnan Applied Basic Research Projects (202302AP370005, 202201AT070196, K264202230211, 202001AV070011), the Yunnan University Startup Program.

Declaration of interests

The authors declare no competing interests.

Main Figure Legends

Figure 1. The stress response is induced in animals fed low-quality food, HK-*E. coli*.

(A) Schematic drawing and quantitative data of the food aversion assay. Circles indicate the food spot for live (yellow) and HK-OP50 (red) bacteria, respectively. The animals were scored 16-17 hours after L1 worms were placed on the food spot. Data are represented as mean ±SD from three independent experiments，79-129 animals/assay.

(B) Schematic method and quantitative data of the food selection assay. Live (yellow), heat-killed (red) *E. coli* and LB as the buffer for *E. coli* were placed on indicated position. Synchronized L1 worms were place in the center spot. The selection index was calculated at the indicated time. Data are represented as

494 mean ±SD from eight independent experiments, 123-792 animals/assay.

495 (C) GO enrichment analysis of up-regulated genes in animals fed with HK-*E.*
496 *coli* vs live *E. coli*.

497 (D) Venn diagram showing numbers of UPR^{ER} target genes and up-regulated
498 genes in animals fed HK-*E. coli*, and their overlap.

499 (E) Venn diagram showing numbers of induction genes by four pathogenic
500 bacteria and HK-*E. coli* induced genes, and their overlap. The gene expression
501 data was extracted from published data of animals' infection with *Pseudomonas*
502 *aeruginosa* (PA) [26], *Bacillus thuringiensis* (Bthu) [27], *Staphylococcus aureus*
503 (Saur) [27], and *Serratia marcescens* (Smar) [27].

504 (F-G) GFP fluorescence images and bar graph showing that *Phsp-4::GFP* (F)
505 and *Pirg-5::GFP* (G) were induced in animals fed with HK-*E. coli.* Blue numbers
506 are the number of worms scored from at least three independent experiments.
507 Data are represented as mean ± SD.

508 For all panels, Scale bar shows on indicated figures, 50 μm. * $p<0.05$, ** $p<0.01$,
509 *** $p < 0.001$, **** $p<0.0001$, ns: no significant difference. Precise P values are
510 provided in Raw Data.

511 **Figure 2. Animals evaluate food quality through UPR^{ER} (*ire-1/xbp-1*) -**
512 **Innate immunity (*pmk-1* MAPK) axis.**

513 (A-B) GFP fluorescence images and bar graph showing that HK-*E. coli* induced
514 *Phsp-4::GFP* was decreased in animals with *ire-1* or *xbp-1* RNAi treatment (A)
515 or *xbp-1* mutation (B). Blue numbers are the number of worms scored from at
516 least three independent experiments. Data are represented as mean ± SD.

517 (C) Food aversion assay showing that *xbp-1* mutation eliminated the
518 discrimination against HK-*E. coli.* However, this effect is rescued by expressing
519 *xbp-1* in neurons rather than intestine. Data are represented as mean ±SD from
520 five independent experiments, 156-763 animals/assay.

521 (D) GFP fluorescence images and bar graph showing that HK-*E. coli* induced
522 *Pirg-5::GFP* was decreased in animals with *pmk-1* RNAi treatment. Blue
523 numbers are the number of worms scored from at least three independent
524 experiments. Data are represented as mean ± SD.

525 (E) Western blot images showing the level of p-PMK-1 in L1 animals (Wild-type
526 N2 and *xbp-1* mutant) fed with OP50 or HK-OP50 for 4 h. The level of p-PMK-
527 1 is induced in animals fed HK-OP50.

528 (F) Food aversion assay showing that *pmk-1* mutation eliminated the
529 discrimination against HK-*E. coli.* However, this effect is rescued by expressing
530 *pmk-1* in neurons rather than intestine. Data are represented as mean ±SD
531 from five independent experiments, 168-492 animals/assay.

532 (G) Food aversion assay in wild-type, *xbp-1*, *pmk-1* and double mutant. Data
533 are represented as mean ±SD from five independent experiments, 259-490
534 animals/assay..

535 For all panels, Scale bar shows on indicated figures, 50 μm. * $p<0.05$, ** $p<0.01$,
536 *** $p < 0.001$, **** $p<0.0001$, ns: no significant difference. Precise P values are
537 provided in Raw Data.

538 **Figure 3. HK-*E. coli* is low sugar food, which induce stress response and**
539 **avoidance behavior in animals.**

540 (A) Food aversion assay showing that wild-type animals eliminated the
541 discrimination against HK-*E. coli* when *yfbR* is mutated in *E. coli*. Data are
542 represented as mean ±SD four independent experiments, 251-490
543 animals/assay.

544 (B) Heat map showing the thirteen differential metabolites from HK-K12, HK-
545 *yfbR*, and K12 in 4 independent experiments. Color indicates the relative level
546 of each metabolite.

547 (C-D) The bar graph showing that HK-*E. coli* induced *Phsp-4::GFP* was

548 decreased in animals with lactose (C) or D-(+)-sucrose (D) supplementation.
549 Blue numbers are the number of worms scored from at least three independent
550 experiments. Data are represented as mean ± SD.

551 (E-F) GFP fluorescence images and bar graph showing that HK-*E. coli* induced
552 *Phsp-4::GFP* (E) and *Pirg-5::GFP* (F) were decreased in animals with D-(+)-
553 glucose (D-Glc) supplementation. Blue numbers are the number of worms
554 scored from at least three independent experiments. Data are represented as
555 mean ± SD.

556 (G) Western blot images showing the level of p-PMK-1 in L1 animals fed HK-*E.*
557 *coli* with or without D-(+)-glucose (D-Glc) supplementation for 4 h. The level of
558 p-PMK-1 is decreased in animals fed HK-OP50+D-Glc.

559 (H) Food aversion assay showing that wild-type animals eliminated the
560 discrimination against HK-*E. coli* with D-Glc supplementation. Data are
561 represented as mean ±SD six independent experiments, 190-492
562 animals/assay.

563 For all panels, Scale bar shows on indicated figures, 50 μm. * $p<0.05$, ** $p<0.01$,
564 *** $p < 0.001$, **** $p<0.0001$, ns: no significant difference. Precise P values are
565 provided in Raw Data.

566

567 **Figure 4. Vitamin C biosynthesis pathway is critically involved in**
568 **evaluating sugar in the food**

569 (A) Cartoon illustration of a simplified, Vitamin C biosynthesis pathway in *C.*
570 *elegans*. The relevant coding genes of enzymes was labeled with red.

571 (B) The level of total L-ascorbic acid (TAA), also known as vitamin C, in animals
572 fed with Live-K12, HK-K12, or HK-*yfbR*. Data are represented as mean ±SD
573 from six independent experiments.

574 (C) The level of total L-ascorbic acid (TAA) in animals (control or knockdown of
575 Vitamin C biosynthesis genes) fed with HK-*E. coli* with or without D-glucuronate

576 (D-GlcA) supplementation. Data are represented as mean ±SD from eight
577 independent experiments.

578 (D-E) GFP fluorescence images and bar graph showing that HK-*E. coli* induced
579 *Phsp-4::GFP* (D) and *Pirg-5::GFP* (E) were decreased in animals with D-GlcA
580 or Vitamin C supplementation. Blue numbers are the number of worms scored
581 from at least three independent experiments. Data are represented as mean ±
582 SD.

583 (F-G) Western blot images showing the level of p-PMK-1 in L1 animals fed with
584 HK-*E. coli* with D-GlcA or Vitamin C supplementation for 4 h. The level of p-
585 PMK-1 is decreased in animals with D-GlcA (F) or Vitamin C (G)
586 supplementation.

587 (H) Food aversion assay showing that wild-type animals eliminated the
588 discrimination against HK-*E. coli* with D-GlcA or Vitamin C supplementation.
589 Data are represented as mean ±SD from four independent experiments, 153-
590 292 animals/assay.

591

592 (I-K) The bar graph showing that suppression of HK-*E. coli* induced *Phsp-*
593 *4::GFP* (I), *Pirg-5::GFP* (J) and food avoidance (K) by D-GlcA supplementation
594 was abolished in animals with RNAi of VC biosynthesis genes, which was not
595 affect by Vitamin C supplementation. Blue numbers are the number of worms
596 scored from at least three independent experiments and Data are represented
597 as mean ±SD(I-J). Data are represented as mean ±SD from five independent
598 experiments, 252-537 animals/assay (K).

599 For all panels, Scale bar shows on indicated figures, 50 μm. * $p<0.05$, ** $p<0.01$,
600 *** $p < 0.001$, **** $p<0.0001$, ns: no significant difference. Precise P values are
601 provided in Raw Data.

602

603 **Figure 5. Animals evaluate sugar and vitamin C through neuronal XBP-1**
604 **and PMK-1**

605 (A) Schematic method of the food selection assay. Food (red) and food with
606 carbohydrate (D-Glc, D-GlcA, or VC) supplementation (green) was placed on
607 indicated position. Synchronized L1 worms were then place in plate. After 16-
608 17hs, the selection index was calculated.

609 (B-D) Food selection assay showing that *xbp-1* or *pmk-1* mutation eliminated
610 the preference of HK-*E. coli* with D-Glc (B), D-GlcA (C) or Vitamin C (D)
611 supplementation, which was rescued in *xbp-1* or *pmk-1* mutant animals by
612 expressing XBP-1 or PMK-1 in neurons rather than intestine.

613 Data are represented as mean ±SD from five independent experiments, 68-647
614 animals/assay (B).

615 Data are represented as mean ±SD from six independent experiments, 83-701
616 animals/assay (C).

617 Data are represented as mean ±SD from six independent experiments, 67-1035
618 animals/assay (D).

619 For all panels, Scale bar shows on indicated figures, 50 μm. * $p<0.05$, ** $p<0.01$,
620 *** $p < 0.001$, **** $p<0.0001$, ns: no significant difference. Precise P values are
621 provided in Raw Data.

622 **Figure 6. Schematic model of physiological food evaluation system in**
623 **evaluating/sensing sugar and vitamin C through UPR^{ER} (IRE-1/XBP-1) -**
624 **Innate immunity (PMK-1/p38 MAPK) axis.**

625 Vitamin C level is low in animals fed low sugar food, HK-*E. coli*. Sugar and
626 Vitamin C deficiency activate cellular UPR^{ER} and immune response, which
627 promote animals to leave low-quality food and seek better food for survival.

628 This cellular stress regulated physiological food evaluation system depends
629 UPR^{ER} (IRE-1/XBP-1) - Innate immunity (PMK-1/p38 MAPK) axis in neuron.

630

631 **Supplemental Figure legends**

632

633 **Figure 1 – figure supplement 1. Food selection assay of animals fed HK-**
634 ***E. coli* or *E. coli.* Relative to Figure 1.**
635 (A-E) Metabolomics analysis of different quality food (HK-K12, HK-*yfbR* and
636 Live-K12). Cluster analysis of all metabolites (A), lipids and their derivatives (B),
637 amino acids and their derivatives (C), coenzymes and vitamins (D), and
638 carbohydrates and their derivatives (E) from Live-K12, HK-K12, and HK-*yfbR*.
639 Color indicates the relative level of each metabolite. HK-K12: heat-killed *E. coli*
640 wild-type K12; HK-*yfbR:* heat-killed *E. coli mutant yfbR;* K12: live *E. coli* wild-
641 type K12. z-score for standardizing data, complete for bi-clustering algorithm,
642 and Euclidean for distance method.
643 (F) Principal component analysis to test the repeatability of the metabolic
644 experiment. HK-K12: heat-killed *E. coli* wild-type K12; HK-*yfbR*: heat-killed *E.*
645 *coli* mutant *yfbR*; K12: live *E. coli* wild-type K12. LB: LB buffer for culturing *E.*
646 *coli.*
647 (G) The number of worms in each position calculated at the indicated time,
648 indicating that animals initially select both foods (1-2h), but eventually favor
649 high-quality food (Live E. coli) until 17h.
650 (H) GO enrichment analysis of UPR^{ER} dependent IRE-1 branch.
651 For all panels, * $p<0.05$, ** $p<0.01$, *** $p < 0.001$, **** $p<0.0001$, ns: no
652 significant difference. Precise P values are provided in Raw Data.

653

654 **Figure 1 – figure supplement 2. Stress response of animals fed HK-*E. coli***
655 **or *E. coli.* Relative to Figure 1.**

656 (A) UPR^{ER} reporter (*Phsp-4::GFP*) and immunity reporter (*Pirg-5::GFP*) were
657 induced in the neuron and intestine of animals fed with HK-*E. coli.* Neurons are
658 highlighted with a red arrow.
659 (B) UPR^{mit} reporter (*Phsp-6::GFP*) was weakly induced in animals fed with HK-
660 *E. coli*.
661 (C) UPR^{ER} reporter (*Phsp-4::GFP*) expression in animals under normal food
662 (OP50), low quality food (HK-OP50), and starved (M9: hatching L1 worm in M9,
663 NGM) condition; L1 animals were cultured in OP50, HK-OP50 or starved NGM
664 for 20h.
665 (D) Immunity reporter (*Pirg-5::GFP*) expression in animals under normal food
666 (OP50), low quality food (HK-OP50), and starved (M9: hatching L1 worm in M9,
667 NGM). L1 animals were cultured in OP50, HK-OP50 or starved NGM for 20h.
668 For all panels, Scale bar shows on indicated figures, 50 μm.
669
670 **Figure 2 - figure supplement 1. UPR^{ER} and innate immunity pathway in**
671 **animals are critical for evaluating HK-*E. coli*. Relative to Figure 2.**
672 (A-B) GFP fluorescence images and bar graph showing that HK-*E. coli* induced
673 *Phsp-4::GFP* was not affected in animals with *atf-4* (A) or *atf-6* (B) RNAi
674 treatment. Blue numbers are the number of worms scored from at least three
675 independent experiments. Data are represented as mean ± SD.
676 (C) qPCR showing that IRE-1-mediated splicing of *xbp-1* mRNA is induced in
677 animals fed with HK-*E. coli.*
678 (D) UPR^{ER} reporter (*Phsp-4::GFP*) expression in animals with candidate RNAi
679 feeding OP50 or HK-OP50.
680 (E) Venn diagram showing the numbers of PMK-1 dependent genes [30] and up-
681 regulated genes in animals fed HK-*E. coli,* and their overlap.
682 (F) The expression of PMK-1 dependent genes which was extracted from RNA-
683 seq data from animals fed with HK-*E. coli*. The data from average of three

684 independent experiments.

685 (G-H) GFP fluorescence images and bar graph showing that *Psysm-1::GFP* (G)
686 and *Pirg-1::GFP* (H) were induced in animals fed HK-*E. coli.* Blue numbers are
687 the number of worms scored from at least three independent experiments. Data
688 are represented as mean ± SD.

689 (I) Immunity reporter (*Pirg-5::GFP*) expression in animals with candidate RNAi
690 feeding OP50 or HK-OP50.

691 For all panels, Scale bar shows on indicated figures, 50 μm. * $p<0.05$, ** $p<0.01$,
692 *** $p < 0.001$, **** $p<0.0001$, ns: no significant difference. Precise P values are
693 provided in Raw Data.

694

695 **Figure 2 - figure supplement 2. UPR^{ER} positively regulates innate**
696 **immunity pathway in animals. Relative to Figure 2.**

697 (A) GFP fluorescence images and bar graph showing that HK-*E. coli* induced
698 *Pirg-5::GFP* was decreased in animals with *ire-1* or *xbp-1* RNAi treatment. Blue
699 numbers are the number of worms scored from at least three independent
700 experiments. Data are represented as mean ± SD.

701 (B) GFP fluorescence images and bar graph showing that *Phsp-4::GFP* was
702 not affected in animals with *pmk-1* RNAi treatment. Blue numbers are the
703 number of worms scored from at least three independent experiments. Data
704 are represented as mean ± SD.

705 (C) Images and bar graph showing that the avoidance behavior of N2, *xbp-1*
706 mutant, and *pmk-1* mutant in response to different food source (*Saprophytic*
707 *staphylococci*-SS, *Pseudomonas aeruginosa*-PA14, or OP50).

708 "Broder" indicates regions with thicker SS boundaries; "In" denotes areas inside
709 SS; "Out" refers to areas without SS. The scale is as follows: 2 for animals
710 capable of escaping from PA14 and feeding on PA14 located with edges; 1 for
711 animals capable of escaping from PA14 but not feeding on PA14 located with

712 edges; 0 for animals unable to escape from PA14 and being killed by PA14.
713 Data are represented as mean ±SD from five independent experiments, 359-
714 670 animals/assay.
715 For all panels, Scale bar shows on indicated figures, 50 μm. * p<0.05, ** p<0.01,
716 *** p < 0.001, **** p<0.0001, ns: no significant difference. Precise P values are
717 provided in Raw Data.
718
719 **Figure 3 - figure supplement 1. *E. coli* Keio mutant screening. Relative to**
720 **Figure 3.**
721 (A) Flow chart of strategy for *E. coli* Keio mutant screening. We identified 20 *E.*
722 *coli* mutants that did not induce *hsp-4::GFP* through the UPR^{ER} reporter (*Pirg-*
723 *5::GFP*) after three rounds of screening (Table S3). From these 20 *E. coli*
724 mutants, we identified 9 *E. coli* mutants that did not induce *Pirg-5::GFP* through
725 the immunity reporter (*Pirg-5::GFP*) screening (Table S3).
726 (B-C) The bar graph showing that HK-*E. coli* induced *Phsp-4::GFP* (B) and *Pirg-*
727 *5::GFP* (C) was decreased in animals fed mutant *E. coli* (Heat-killed). Blue
728 numbers are the number of worms scored from at least three independent
729 experiments. Data are represented as mean ± SD.
730 For all panels, * p<0.05, ** p<0.01, *** p < 0.001, **** p<0.0001, ns: no
731 significant difference. Precise P values are provided in Raw Data.
732
733 **Figure 3 - figure supplement 2. Low sugar food, HK-*E. coli*, induce stress**
734 **response and avoidance behavior in animals. Relative to Figure 3.**
735 (A) Venn diagram showing the number of differentially metabolites in HK-*E. coli*-
736 K12, HK-*E. coli-yfbR* and *E. coli*.
737 (B) KEGG enrichment analysis of differentially expressed genes in animals fed
738 HK-*E. coli* vs live *E. coli*. We noticed that most of glycolysis/gluconeogenesis
739 genes are up-regulated in animals fed HK-*E. coli*.

740 (C) The bar graph showing that HK-E. coli induced *Phsp-4::GFP* was not
741 affected in animals with D-(+)-trehalose supplementation. Blue numbers are the
742 number of worms scored from at least three independent experiments. Data
743 are represented as mean ± SD.
744 (D) GFP fluorescence images and bar graph showing that HK-*E. coli* induced
745 *Psysm-1::GFP* was decreased in animals with D-(+)-glucose (D-Glc)
746 supplementation. Blue numbers are the number of worms scored from at least
747 three independent experiments. Data are represented as mean ± SD.
748 (E) UPR^{ER} reporter (*Phsp-4::GFP*) expression animals with D-Glc
749 supplementation under OP50, HK-OP50, or NGM condition.
750 (F) immunity reporter (*Pirg-5::GFP*) expression animals with D-Glc
751 supplementation under OP50, HK-OP50, or NGM condition.
752 (G) Development of animals after 48h fed with OP50, HK-OP50, HK-OP50+D-
753 Glc, and HK-OP50+D-GlcA. Blue numbers are the number of worms scored
754 from at least three independent experiments. Data are represented as mean
755 ± SD.
756 For all panels, Scale bar shows on indicated figures, 50 μm. * $p<0.05$, ** $p<0.01$,
757 *** $p < 0.001$, **** $p<0.0001$, ns: no significant difference. Precise P values are
758 provided in Raw Data.
759
760 **Figure 4 - figure supplement 1. Vitamin C biosynthesis pathway is**
761 **critical for evaluating low sugar. Relative to Figure 4.**
762 (A) The level of total L-ascorbic acid (TAA) in Live-K12, HK-K12, or HK-*yfbR*.
763 Data are represented as mean ±SD from six independent experiments.
764 (B) The level of total L-ascorbic acid (TAA) in animals fed HK-*E. coli* with or
765 without D-Glc supplementation. Data are represented as mean ±SD from eight
766 independent experiments.
767 (C) GFP fluorescence images and bar graph showing that HK-*E. coli* induced

768 *Psysm-1::GFP* was decreased in animals with D-GlcA or vitamin C
769 supplementation. Blue numbers are the number of worms scored from at least
770 three independent experiments. Data are represented as mean ± SD.
771 (D) The bar graph showing that suppression of HK-*E. coli* induced *Psysm-*
772 *1::GFP* by D-GlcA supplementation was abolished in animals with RNAi of VC
773 biosynthesis genes, which was not affect by vitamin C supplementation. Blue
774 numbers are the number of worms scored from at least three independent
775 experiments. Data are represented as mean ±SD.
776 (E) Food selection assay showing that the preference of HK-*E. coli* with D-GlcA
777 supplementation was abolished in animals by RNAi of vitamin C biosynthesis
778 genes. Data are represented as mean ±SD from six independent experiments,
779 427-775 animals/assay.
780 For all panels, Scale bar shows on indicated figures, 50 μm. * $p<0.05$, ** $p<0.01$,
781 *** $p < 0.001$, **** $p<0.0001$, ns: no significant difference. Precise P values are
782 provided in Raw Data.
783
784 **Figure 5 - figure supplement 1. Food behavior of animals. Relative to**
785 **Figure 5.**
786 (A) Food selection assay for OP50 & OP50 + D-Glc, D-GlcA, or VC, respectively.
787 Data are represented as mean ±SD from five independent experiments, 241-
788 1182 animals/assay.
789 (B) Food selection assay for buffer (H_2O) & buffer (H_2O) + D-Glc, D-GlcA, or
790 VC, respectively. Data are represented as mean ±SD from five independent
791 experiments, 8-153 animals/assay.
792 (C) Food avoidance assay for N2 & kgb-1 mutant animals fed with HK-*E. coli*.
793 Data are represented as mean ±SD from six independent experiments, 348-
794 660 animals/assay.
795 (D) Translation ability of animals fed with OP50 or HK-OP50 are presented by

796 Western blot of puromycin-labeled peptides.

797 For all panels, * $p<0.05$, ** $p<0.01$, *** $p < 0.001$, **** $p<0.0001$, ns: no
798 significant difference. Precise P values are provided in Raw Data.

799

800 **Supplemental Tables:**

801 **Table S1.** Metabolices analysis.

802 **Table S2.** RNA-seq analysis.

803 **Table S3.** Screening data for *E. coli* mutant keio library.

804 **Table S4.** Metabolomics-seq data of HK-K12, HK-*yfbR* and K12.

805 **Table S5.** RNA-seq data of animals fed with HK-*E. coli* OP50 and *E. coli* OP50.

806 **Raw-data.** Raw data for experiments.

807

808 **Star Methods**

809

810 **Resource Availability**

811

812 **Lead contact**

813 Further information and requests for reagents may be directed to the lead
814 contact Bin Qi (qb@yun.edu.cn).

815

816 **Materials availability**

817 All reagents and strains generated by this study are available through request
818 to the lead contact with a completed Material Transfer Agreement.

819

820 **Data and code availability**

821 Metabolomics-seq data are accessible in Table S4

822 RNA-seq data are accessible in Table S5.

823 This paper does not report original code.

824 Any additional information required to reanalyze the data reported in this paper
825 is available from the lead contact upon request.
826
827 **Experimental model and subject details**
828
829 ***C. elegans* strains and maintenance**

830 Nematode stocks were maintained on nematode growth medium (NGM)
831 plates seeded with bacteria (*E. coli OP50*) at 20℃.

832 1) The following strains/alleles were obtained from the Caenorhabditis
833 Genetics Center (CGC) or as indicated:

834 N2 Bristol (wild type control strain);

835 AU78: *agIs219 [T24B8.5p::GFP::unc-54 3' UTR + Pttx-3::GFP::unc-54 3'*
836 *UTR]*;

837 SJ4005: *zcIs4 [Phsp-4::GFP]*;

838 AY101: *acIs101 [F35E12.5p::GFP + rol-6(su1006)]*;

839 SJ17: *xbp-1 (zc12)*;

840 KU25: *pmk-1(km25)*;

841 AY102: *pmk-1(km25) IV; acEx102 [Pvha-6::pmk-1::GFP + rol-6(su1006)]*;

842 YNU108: *Ex[Prgef-1::pmk-1::GFP，Podr-1::RFP]*[35];

843 *xbp-1(tm2482)* [56];

844 KU21：*kgb-1(km21)*;

845 AU133: *agIs17 [Pmyo-2::mCherry + Pirg-1::GFP] IV*;

846 SJ4100: *zcIs13 [Phsp-6::GFP + lin-15(+)]*.

847 2)The following strains were constructed by this study:

848 YNU242: *xbp-1(tm2482); pmk-1(km25)* double mutant was constructed by
849 crossing: *xbp-1(tm2482)* with KU25[*pmk-1(km25)*].

850 YNU240: *ylfEx149 [xbp-1(tm2482); Prgef-1::xbp-1::GFP; Podr-1::RFP]*
851 transgene strain was constructed by injecting plasmid *Prgef-1::xbp-1::GFP*
852 with *Podr-1::RFP* in *xbp-1(tm2482)* background

853 YNU241: *ylfEx150 [xbp-1(tm2482); Pges-1::xbp-1::GFP; Podr-1::RFP]*
854 transgene strain was constructed by injecting plasmid P*ges-1:xbp-1::GFP* with
855 *Podr-1::RFP* in *xbp-1(tm2482)* background

856

857 **Bacterial strains**

858 *E. coli*-OP50, *Saprophytic staphylococci*, *Pseudomonas aeruginosa-PA14*, *E.*
859 *coli*-K12 (BW25113), and *E. coli*-K12 mutant were cultured at 37˚C in LB
860 medium. A standard overnight cultured bacteria was then spread onto each
861 Nematode growth media (NGM) plate.

862

863 **Culture Medium**

864 MGN Medium：Sigma agar: 20g/L; Bacto Peptone: 2.5g/L; NaCl: 3g/L;
865 MgSO4: 0.12g/L; CaCl: 0.111g/L; PPB:（KH2PO4 0.8M; K2HPO4 • 3H2O
866 0.2M）25ml/L; Cholesterol: 0.005g/L.

867 LB broth: TPYPTONE: 10g/L; Yeast Extract: 5g/L; NaCl 5g/L.

868

869 **Method Details**

870

871 **Generation of transgenes**

872 1）To construct the *C. elegans* plasmid for expression of *xbp-1* in neuron,
873 3057bp promoter of *rgef-1* and genomic DNA of *xbp-1* was inserted into the
874 PPD95.77 vector. DNA plasmid mixture containing *Prgef-1::xbp-1::GFP*
875 (25ng/ul) and *Podr-1::RFP* (25ng/ul) was injected into the gonads of adult
876 *xbp-1(tm2482)*.
877 2）To construct the *C. elegans* plasmid for expression of *xbp-1* in intestine,
878 2549 bp promoter of ges-1 and genomic DNA of *xbp-1* was inserted into the
879 PPD95.77 vector. DNA plasmid mixture containing *Pges-1::xbp-1::GFP*
880 (25ng/ul) and *Podr-1::RFP (25ng/ul)* was injected into the gonads of adult
881 *xbp-1(tm2482)*.

882

883 **Preparation and feeding of worm food**

884 We followed an established protocol [24, 25] to prepare heat-killed (HK) *E. coli*.
885 Briefly, a standard OD_{600}=0.5-0.6 of *E. coli* OP50 and *E. coli* K12 grown in LB
886 broth was concentrated to 1/20 vol and was then heat-killed at 80℃ for 180
887 min. About 150ul of the heat-killed bacteria was spread onto each 35mm
888 NGM plate.

889

890 **Preparation of HK-*E. coli* + carbohydrate or vitamin C food**

1) 100ul of water, 100ul of L-ascorbic acid (dissolved in water at a concentration of 100mg/ml, Sangon Biotech, 100143-0100) or 100 ul of D-glucuronic acid (dissolved in water at a concentration of 100mg/ml，Adamas, 1102520) was mixed with 500 ul of HK-*E. coli*, then 150ul of the mixture was spread onto 35mm NGM plates.

2) 12.5ul of water or 12.5ul of D-(+)-glucose (dissolved in water at a concentration of 100mg/ml, Sangon Biotech, A501991-0500) was mixed with 500 ul of HK-*E. coli*, then 150ul of the mixture was spread onto 35mm NGM plates.

Behavioral assay

***C. elegans* selection assays**

For *C. elegans* to have enough space to evaluate food, we add 18ul of the sample onto a 35mm NGM plate. This creates a round lawn with a radius of 5mm, which occupies about 8% of the total plate area.

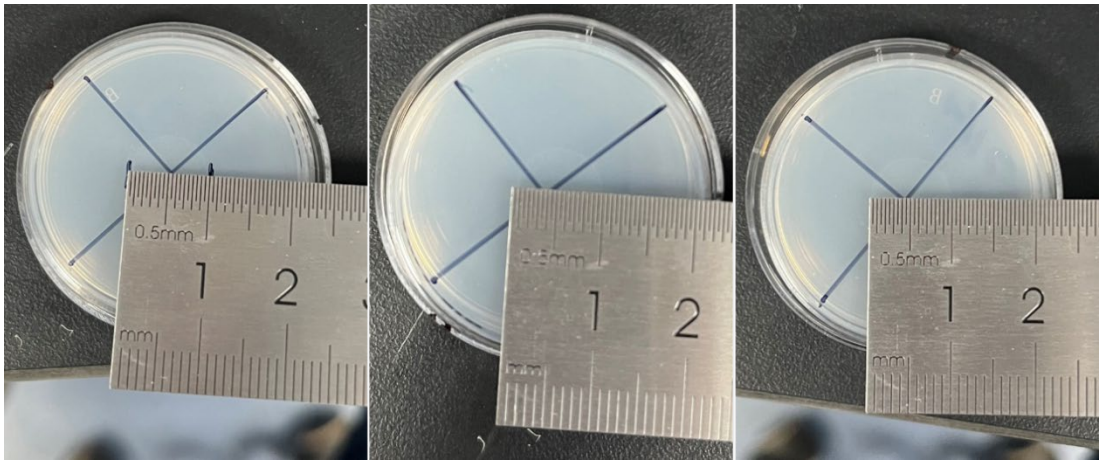

$$\frac{a}{b} = \frac{\pi r_1^2}{\pi \gamma_2^2} = \frac{5mm^2}{17.5mm^2} = 8\%$$

a: the area of bacterial lawn
b: the space of worm life (area of culture dish)

1) 18ul of heat-killed OP50, live OP50, and LB broth (as the buffer for bacteria) was added into 35mm NGM plate in an equilateral triangle pattern. Then, synchronized L1 worms were seeded in the center of NGM plate for 16-17h at 20℃ (as indicated in Figure1B).

2) 18ul of heat-killed OP50 and heat-killed OP50 with D-GlcA or vitamin C was added into 35mm NGM plate in an equilateral triangle pattern, then synchronized L1 worms were seeded on equilateral triangle of NGM plate for 16-17h at 20℃ (as indicated in Figure 5A).

Here is Selection rate formula:

$$selection\ rate = \frac{\frac{worm\ amount}{one\ lawn\ area}}{\frac{worm\ amount}{lawn1\ area} + \frac{worm\ amount}{lawn2\ area} + \frac{worm\ amount}{lawn3\ area} \cdots}$$

***C. elegans* aversion assays**

18ul food was spread out the center of NGM plate, then synchronized L1 by bleach solution (NaOH: 1M, NaClO:4-6%) worms were seeded on center of food for 16-17h at 20 ℃.

$$\text{Aversion index} = \frac{worm\ amount\ of\ out\ \text{of}\ lawn}{worm\ amount\ of\ (out + in)\ \ lawn}$$

927 Three to ten replicates for each condition were performed for each assay, and
928 the experiments were duplicated on different days.

929

930 **Analysis of the fluorescence intensity in worms**

931 The synchronized L1 worms carrying either UPR^{ER} reporter (*Phsp-4::GFP*) or
932 innate immunity reporter (*Pirg-5::GFP*; *Psysm-1p::GFP*; *Pirg-1p::GFP*) were
933 seeded on NGM with indicated food and incubated for 24h at 20℃. For
934 fluorescence imaging, worms were anesthetized with 25 mM levamisole and
935 photographed using either an Olympus BX53 microscope or Olympus MVX10
936 dissecting microscope equipped with a DP80 camera.

937 The fluorescence intensity in entire intestinal region was quantified using
938 ImageJ software and normalized to the body area.

939

940 ***E. coli* Keio collection screen**

941 The whole Keio *E. coli* single mutant collection (Baba et al., 2006) was
942 screened. Mutant bacteria strains, as well as the wild-type control strain
943 BW25113, were cultured in LB medium with 50μg/ml kanamycin at 37℃ until
944 an OD_{600} of 0.5-0.6 was reached. The bacteria were then heat-killed following
945 our established protocol [24], and 150 ul of the heat-killed mutant *E. coli* was
946 spread onto 35 mm NGM plates. Synchronized L1 worms carrying UPR^{ER}
947 reporter (*Phsp-4::GFP*) were seeded and cultured for 24h at 20℃. The
948 fluorescence was then examined by using an Olympus MVX10 dissecting
949 microscope, progressive screening three times. Next, a 4th screen was
950 performed using immune reporter (*Pirg-5::GFP*) animals fed with HK-E. coli

951 mutants that reduced the *Phsp-4::GFP* fluorescence. Finally, an aversion
952 behavior assay was performed using HK-*E. coli* mutants that both reduced
953 *Phsp-4::GFP* and *Pirg-5::GFP.* HK-*E. coli* mutants that reduced UPR^{ER},
954 immune and avoidance behavior were identified through this screening.

955

956 **RNAi treatment**

957 RNAi plasmid is delivered in a *E. coli* strain, HT115, from either the MRC
958 RNAi library [57] or the ORF-RNAi Library [58]. RNAi plates were prepared by
959 adding IPTG to NGM agar to a final concentration of 1 mM. Overnight *E. coli*
960 cultures (LB broth containing 100 ug/ml ampicillin and 100uM IPTG) of
961 specific RNAi strains and the control HT115 strain were seeded onto RNAi
962 feeding plates and cultured at room temperature until dry. Synchronized L1
963 worms were treated RNAi by feeding (Ahringer, Reverse genetics, WormBook
964 2006) for the first generation and allowed to grow to maturity. The worms
965 were then bleached and hatched in M9 buffer for 18hr. The synchronized L1
966 worms were then seeded on the indicated feeding plate.

967

968 **Western blot**

969 To measure the level of p-PMK-1, worms (feeding different food for 4h) were
970 analyzed by standard western blot methods and probed with anti-p38 (dilution
971 = 1:5,000; Cell Signaling, 9212S), anti-p-p38 (dilution = 1:5,000; Cell
972 Signaling, 4511S) and anti-α-tubulin (dilution = 1:10,000; Sigma T5168) as a
973 loading control.

974 To measure the level of protein translation, worms (feeding different food for
975 24h) were analyzed by standard western blot methods and probed with anti-
976 Puromycin (dilution = 1:10,000; Sigma-Aldrich, MABE343) and anti-α-tubulin
977 (dilution = 1:10,000; Sigma T5168) as a loading control.

978

979 **Total content of ascorbic acid (TAA) assay**

980 The total content of ascorbic acid was measured using the kits (Beijing
981 Biotech-Pack-analytical Scientific Co., Ltd., Beijing, China, BKWB132
982 http://biotech-pack-analytical.foodmate.net/) according to the manufacturer's
983 protocol. Briefly, L1 worms were seeded on the different feeding assay plate
984 and cultured for 4 hours. The worms were then lysed in ice-cold conditions
985 using lysis buffer. Equal amounts of protein were used for the normalization.
986 Here is formula for getting TAA concentration

987 $$\mathrm{TAA(ug/mg\ prot)} = ((\triangle \mathrm{A} - \mathrm{a}) \div \mathrm{b})) \div (\mathrm{Cpr} \times \mathrm{V1}) \times \mathrm{D}$$

988 V1 - the volume of supernatant of for experiment

989 Cpr – the concentration of supernatant protein

990 D – Dilution ratio of supernatant

991 a – the intercept of standard curve

992 b – the slope of standard curve

993 the standard curve y = 0.0611x + 0.0003 for Figure 4C; y = 0.0258x + 0.0066
994 for Figure 4B, Figure 4-figure supplement 1A and Figure 4-figure supplement
995 1B.

996

997 **Preparation of samples for RNA sequencing**

998 RNA-seq was done with three biological replicates that were independently
999 generated, collected, and processed. Adult wild type (N2) worms were
1000 bleached and then the eggs were incubated in M9 for 18 hours to obtain
1001 synchronized L1 worms. L1 worms were cultured in the NGM plate with *HK-E.*
1002 *coli* or *E. coli* for 4hrs at 20℃. L1 worms were then collected for sequencing.

1003

1004 **RNA sequencing and data processing**

1005 For the RNA sequencing assay, cDNA libraries were constructed, and single-
1006 end libraries were sequenced using the Illumina platform (Novogene, Beijing,
1007 China). HISAT2 [59] was used to map the clean reads to the reference gene
1008 sequence (Species: Caenorhabditis_elegans; Source: NCBI; Reference
1009 Genome Version: GCF_000002985.6_WBcel235), and then “featureCounts”
1010 tool in subread software [60] was used to calculate the gene expression level of
1011 each sample. Read counts were inputted into DESeq2 [61]to calculate
1012 differential gene expression and statistical significance. Differentially
1013 expressed genes (DEGs) were screened using following criteria:
1014 |log2(FoldChange)| > 1 & padj<= 0.05.

1015

1016 **Preparation of samples for metabolome sequencing**

1017 Metabolome-seq of bacterial was done with four biological replicates that
1018 were independently generated, collected, and processed. Total of three group
1019 E. coli sample including: *E. coli K12* (Con), HK-*E. coli K12* (HK), and HK-*E.*

1020 *coli yfbR* mutant (HY). All bacteria were overnight cultured to the same OD
1021 (OD_{600}=1). *E. coli K12* and *E. coli yfbR* mutant are heat-killed (80, 180min), *E.*
1022 *coli* K12, HK-*E. coli* K12 and HK-*E. coli yfbR* mutant were then spread out
1023 NGM plate for 72hs at room temperature. Finally, sample was collected into
1024 1.5ml tube by using sterile cell scraping.

1025

1026 **Metabolome sequencing and data processing**

1027 Metabolome were sequenced using the Ultra Performance Liquid
1028 Chromatography (UPLC) (ExionLC AD，https://sciex.com.cn/) and Quadrupole-
1029 Time of Flight (TripleTOF 6600, AB SCIEX) for Non-targeted; Ultra Performance
1030 Liquid Chromatography (UPLC) (ExionLC AD， https://sciex.com.cn/) and
1031 Tandem mass spectrometry（MS/MS）（QTRAP®，https://sciex.com/）for Broad
1032 targeting (Metware, Wuhan, China). Multiple reaction monitoring (MRM) was
1033 used to calculate the expression level of each metabolite. Differential
1034 metabolites were screened through Fold change ⩾ 2 or Fold change ⩽ 0.5
1035 and VIP ⩾ 1 (Variable Importance in Projection of OPLS-DA model).

1036

1037 **Microscopy**

1038 Analysis of fluorescence was performed with an Olympus BX53 microscope,
1039 CLSM (Zeiss LSM900), or Olympus MVX10 dissecting with a DP80 camera.

1040

1041 **QUANTIFICATION AND STATISTICAL ANALYSIS**

1042 **Quantification**

1043 ImageJ software was used for quantifying fluorescence intensity of UPR^{ER}
1044 and Innate immunity reporter. ImageJ software was used for counting the
1045 number of worms about selection and aversion behavior.

1046

1047 **Statistical analysis**

1048 All statistical analyses were performed in Graphpad prism 8.0. Two-tailed
1049 unpaired t test was used for statistical analysis of two groups of samples，
1050 one-way or two-way ANOVA was used for statistical analysis of more than
1051 two groups of samples. Data are presented as Mean ± SD, and $p<0.05$ was
1052 considered a significant difference, "*" represents $p<0.05$, "**" represents
1053 $p<0.01$, "***" is represents < 0.001, "****" represents $p<0.0001$,
1054 "ns" represents no significant difference. For all figures, ''n'' represents the
1055 number of worms scored from at least three independent experiments.

1056

1057 **Reference:**

1058 1. Filosa A, Barker AJ, Dal Maschio M, Baier H. Feeding State Modulates
1059 Behavioral Choice and Processing of Prey Stimuli in the Zebrafish Tectum.
1060 *Neuron* **90**, 596-608 (2016).
1061
1062 2. Florsheim EB, Sullivan ZA, Khoury-Hanold W, Medzhitov R. Food allergy as a
1063 biological food quality control system. *Cell* **184**, 1440-1454 (2021).
1064
1065 3. McLachlan IG*, et al.* Diverse states and stimuli tune olfactory receptor
1066 expression levels to modulate food-seeking behavior. *Elife* **11**, (2022).
1067
1068 4. Avery JA, Liu AG, Ingeholm JE, Gotts SJ, Martin A. Viewing images of foods
1069 evokes taste quality-specific activity in gustatory insular cortex. *Proc Natl*
1070 *Acad Sci U S A* **118**, (2021).
1071
1072 5. Melin AD*, et al.* Fruit scent and observer colour vision shape food-selection

strategies in wild capuchin monkeys. *Nat Commun* **10**, 2407 (2019).

6. Bargmann CI. Chemosensation in C. elegans. *WormBook*, 1-29 (2006).

7. Sengupta P, Chou JH, Bargmann CI. odr-10 encodes a seven transmembrane domain olfactory receptor required for responses to the odorant diacetyl. *Cell* **84**, 899-909 (1996).

8. Troemel ER, Kimmel BE, Bargmann CI. Reprogramming chemotaxis responses: sensory neurons define olfactory preferences in C. elegans. *Cell* **91**, 161-169 (1997).

9. Fiala A. Olfaction and olfactory learning in Drosophila: recent progress. *Curr Opin Neurobiol* **17**, 720-726 (2007).

10. Chalasani SH*, et al.* Dissecting a circuit for olfactory behaviour in Caenorhabditis elegans. *Nature* **450**, 63-70 (2007).

11. Zhang B, Jun H, Wu J, Liu J, Xu XZS. Olfactory perception of food abundance regulates dietary restriction-mediated longevity via a brain-to-gut signal. *Nat Aging* **1**, 255-268 (2021).

12. Ha HI*, et al.* Functional organization of a neural network for aversive olfactory learning in Caenorhabditis elegans. *Neuron* **68**, 1173-1186 (2010).

13. Scott K. Gustatory Processing in Drosophila melanogaster. *Annu Rev Entomol* **63**, 15-30 (2018).

14. Hukema RK, Rademakers S, Dekkers MP, Burghoorn J, Jansen G. Antagonistic sensory cues generate gustatory plasticity in Caenorhabditis elegans. *Embo J* **25**, 312-322 (2006).

15. Ni L*, et al.* A gustatory receptor paralogue controls rapid warmth avoidance in Drosophila. *Nature* **500**, 580-584 (2013).

16. Jones D, Candido EPM. Feeding is inhibited by sublethal concentrations of toxicants and by heat stress in the nematode Caenorhabditis elegans: Relationship to the cellular stress response. *J Exp Zool* **284**, 147-157 (1999).

17. Xie Z*, et al.* The gut-to-brain axis for toxin-induced defensive responses. *Cell* **185**, 4298-4316 e4221 (2022).

18. Richardson CE, Kooistra T, Kim DH. An essential role for XBP-1 in host

1116 protection against immune activation in C. elegans. *Nature* **463**, 1092-1095
1117 (2010).
1118
1119 19. Kim DH*, et al.* A conserved p38 MAP kinase pathway in Caenorhabditis
1120 elegans innate immunity. *Science* **297**, 623-626 (2002).
1121
1122 20. Carr AC, Maggini S. Vitamin C and Immune Function. *Nutrients* **9**, (2017).
1123
1124 21. Steinert RE, Lee YK, Sybesma W. Vitamins for the Gut Microbiome. *Trends Mol*
1125 *Med* **26**, 137-140 (2020).
1126
1127 22. Li Y, Schellhorn HE. New developments and novel therapeutic perspectives for
1128 vitamin C. *J Nutr* **137**, 2171-2184 (2007).
1129
1130 23. Carr AC, Frei B. Toward a new recommended dietary allowance for vitamin C
1131 based on antioxidant and health effects in humans. *Am J Clin Nutr* **69**, 1086-
1132 1107 (1999).
1133
1134 24. Qi B, Kniazeva M, Han M. A vitamin-B2-sensing mechanism that regulates gut
1135 protease activity to impact animal's food behavior and growth. *eLife* **6**,
1136 e26243 (2017).
1137
1138 25. Qi B, Han M. Microbial Siderophore Enterobactin Promotes Mitochondrial
1139 Iron Uptake and Development of the Host via Interaction with ATP Synthase.
1140 *Cell* **175**, 571-582.e511 (2018).
1141
1142 26. Nakad R*, et al.* Contrasting invertebrate immune defense behaviors caused by
1143 a single gene, the Caenorhabditis elegans neuropeptide receptor gene npr-1.
1144 *BMC Genomics* **17**, 280 (2016).
1145
1146 27. Sinha A, Rae R, Iatsenko I, Sommer RJ. System wide analysis of the evolution
1147 of innate immunity in the nematode model species Caenorhabditis elegans
1148 and Pristionchus pacificus. *PLoS One* **7**, e44255 (2012).
1149
1150 28. Calfon M*, et al.* IRE1 couples endoplasmic reticulum load to secretory
1151 capacity by processing the XBP-1 mRNA. *Nature* **415**, 92-96 (2002).
1152
1153 29. Bolz DD, Tenor JL, Aballay A. A Conserved PMK-1/p38 MAPK Is Required in
1154 Caenorhabditis elegans Tissue-specific Immune Response to Yersinia pestis
1155 Infection*. *The Journal of Biological Chemistry* **285**, 10832 - 10840 (2010).
1156
1157 30. Yoneda T, Benedetti C, Urano F, Clark SG, Harding HP, Ron D. Compartment-
1158 specific perturbation of protein handling activates genes encoding

1159 mitochondrial chaperones. *Journal of Cell Science* **117**, 4055-4066 (2004).
1160
1161 31. Hetz C, Zhang K, Kaufman RJ. Mechanisms, regulation and functions of the
1162 unfolded protein response. *Nat Rev Mol Cell Biol* **21**, 421-438 (2020).
1163
1164 32. Ron D, Walter P. Signal integration in the endoplasmic reticulum unfolded
1165 protein response. *Nat Rev Mol Cell Biol* **8**, 519-529 (2007).
1166
1167 33. Fletcher M, Tillman EJ, Butty VL, Levine SS, Kim DH. Global transcriptional
1168 regulation of innate immunity by ATF-7 in C. elegans. *Plos Genet* **15**, (2019).
1169
1170 34. Foster KJ, McEwan DL, Pukkila-Worley R. Measurements of Innate Immune
1171 Function in C. elegans. *Methods Mol Biol* **2144**, 145-160 (2020).
1172
1173 35. Geng S*, et al.* Gut commensal E. coli outer membrane proteins activate the
1174 host food digestive system through neural-immune communication. *Cell Host*
1175 *Microbe* **30**, 1401-1416 e1408 (2022).
1176
1177 36. Weiss B. The Deoxycytidine Pathway for Thymidylate Synthesis in
1178 Escherichia coli. *Journal of Bacteriology* **189**, 7922-7926 (2007).
1179
1180 37. Franceus J, Desmet T. Sucrose Phosphorylase and Related Enzymes in
1181 Glycoside Hydrolase Family 13: Discovery, Application and Engineering.
1182 *International Journal of Molecular Sciences* **21**, (2020).
1183
1184 38. Xing S*, et al.* Lactose induced redox-dependent senescence and activated Nrf2
1185 pathway. *Int J Clin Exp Pathol* **12**, 2034-2045 (2019).
1186
1187 39. Patananan AN, Budenholzer LM, Pedraza ME, Torres ER, Adler LN, Clarke SG.
1188 The invertebrate Caenorhabditis elegans biosynthesizes ascorbate. *Arch*
1189 *Biochem Biophys* **569**, 32-44 (2015).
1190
1191 40. Yabuta Y*, et al.* L-Ascorbate Biosynthesis Involves Carbon Skeleton
1192 Rearrangement in the Nematode Caenorhabditis elegans. *Metabolites* **10**,
1193 (2020).
1194
1195 41. Moritz B, Schmitz AE, Rodrigues ALS, Dafre AL, Cunha MP. The role of vitamin
1196 C in stress-related disorders. *The Journal of Nutritional Biochemistry* **85**,
1197 (2020).
1198
1199 42. Rice ME. Ascorbate regulation and its neuroprotective role in the brain.
1200 *Trends in Neurosciences* **23**, 209-216 (2000).
1201

43. Webb AL, Villamor E. Update: Effects of Antioxidant and Non-Antioxidant Vitamin Supplementation on Immune Function. *Nutrition Reviews* **65**, 181-217 (2007).

44. Maggini S, Wintergerst ES, Beveridge S, Hornig DH. Selected vitamins and trace elements support immune function by strengthening epithelial barriers and cellular and humoral immune responses. *British Journal of Nutrition* **98**, S29-S35 (2007).

45. Luo X*, et al.* Vitamin C protects against hypoxia, inflammation, and ER stress in primary human preadipocytes and adipocytes. *Molecular and Cellular Endocrinology* **556**, (2022).

46. Su M, Liang X, Xu X, Wu X, Yang B. Hepatoprotective benefits of vitamin C against perfluorooctane sulfonate-induced liver damage in mice through suppressing inflammatory reaction and ER stress. *Environmental Toxicology and Pharmacology* **65**, 60-65 (2019).

47. Ozbey NP*, et al.* Tyramine Acts Downstream of Neuronal XBP-1s to Coordinate Inter-tissue UPR(ER) Activation and Behavior in C. elegans. *Dev Cell* **55**, 754-770 e756 (2020).

48. Troemel ER, Chu SW, Reinke V, Lee SS, Ausubel FM, Kim DH. p38 MAPK regulates expression of immune response genes and contributes to longevity in C. elegans. *Plos Genet* **2**, e183 (2006).

49. Melo JA, Ruvkun G. Inactivation of conserved C. elegans genes engages pathogen- and xenobiotic-associated defenses. *Cell* **149**, 452-466 (2012).

50. Kaser A*, et al.* XBP1 links ER stress to intestinal inflammation and confers genetic risk for human inflammatory bowel disease. *Cell* **134**, 743-756 (2008).

51. Kaser A, Blumberg RS. Survive an innate immune response through XBP1. *Cell Research* **20**, 506-507 (2010).

52. Guan L, Zhan Z, Yang Y, Miao Y, Huang X, Ding M. Alleviating chronic ER stress by p38-Ire1-Xbp1 pathway and insulin-associated autophagy in C. elegans neurons. *PLOS Genetics* **16**, e1008704 (2020).

53. Qu M, Liu Y, Xu K, Wang D. Activation of p38 MAPK Signaling‐Mediated Endoplasmic Reticulum Unfolded Protein Response by Nanopolystyrene Particles. *Advanced Biosystems* **3**, 1800325 (2019).

54. Weaver BP, Weaver YM, Omi S, Yuan W, Ewbank JJ, Han M. Non-Canonical Caspase Activity Antagonizes p38 MAPK Stress-Priming Function to Support Development. *Dev Cell* **53**, 358-369 e356 (2020).

55. Ozbey NP, Thompson MA, Taylor RC. The regulation of animal behavior by cellular stress responses. *Exp Cell Res* **405**, 112720 (2021).

56. Richardson CE, Kinkel S, Kim DH. Physiological IRE-1-XBP-1 and PEK-1 signaling in Caenorhabditis elegans larval development and immunity. *PLoS Genet* **7**, e1002391 (2011).

57. Kamath RS*, et al.* Systematic functional analysis of the Caenorhabditis elegans genome using RNAi. *Nature* **421**, 231-237 (2003).

58. Rual JF*, et al.* Toward improving Caenorhabditis elegans phenome mapping with an ORFeome-based RNAi library. *Genome Res* **14**, 2162-2168 (2004).

59. Mortazavi A, Williams BA, McCue K, Schaeffer L, Wold B. Mapping and quantifying mammalian transcriptomes by RNA-Seq. *Nat Methods* **5**, 621-628 (2008).

60. Liao Y, Smyth GK, Shi W. featureCounts: an efficient general purpose program for assigning sequence reads to genomic features. *Bioinformatics* **30**, 923-930 (2014).

61. Love MI, Huber W, Anders S. Moderated estimation of fold change and dispersion for RNA-seq data with DESeq2. *Genome Biol* **15**, (2014).

Figure 1

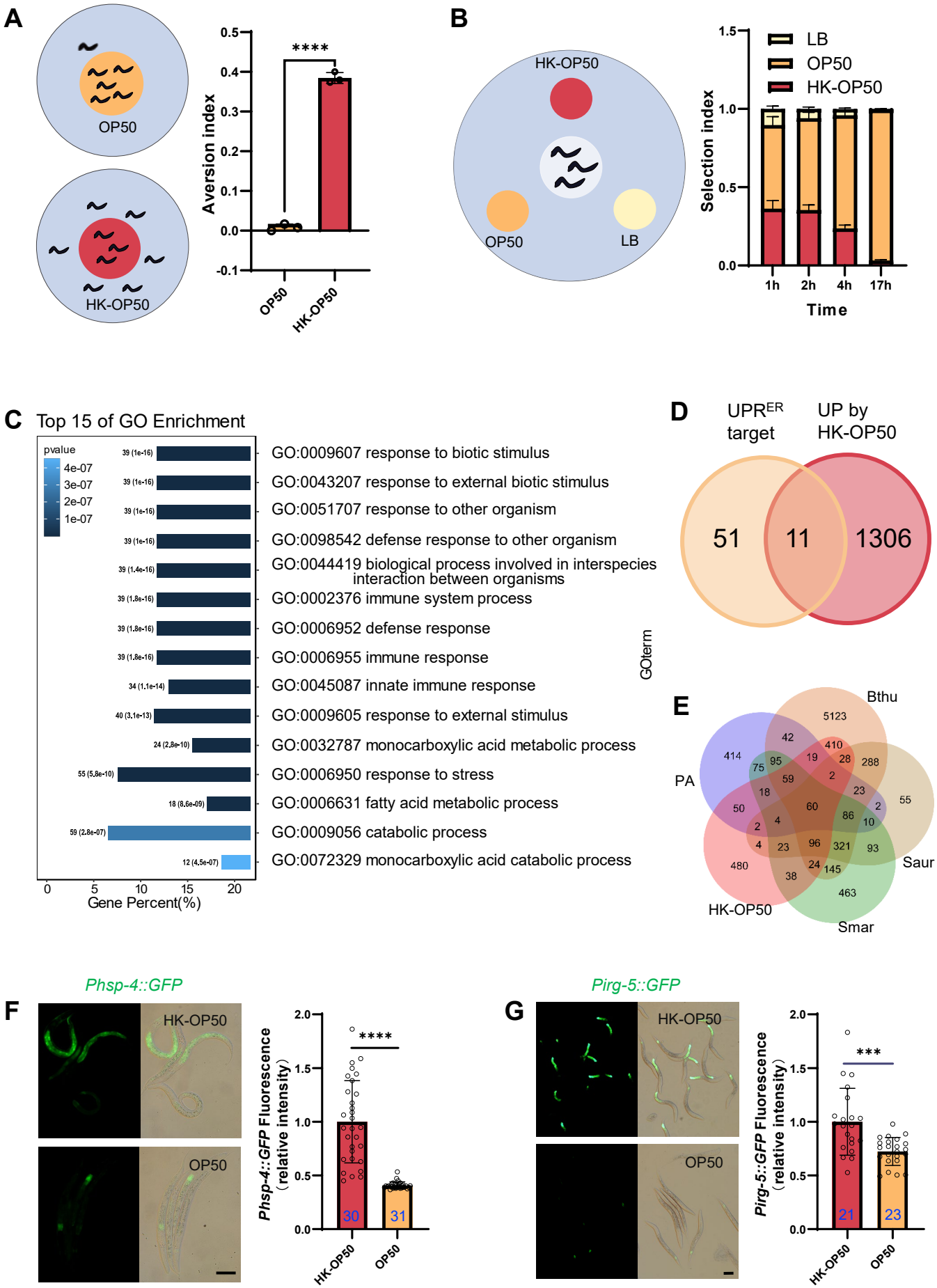
A
OP50
HK-OP50
Aversion index
****
OP50
HK-OP50
B
HK-OP50
OP50
LB
LB
OP50
HK-OP50
Selection index
1h
2h
4h
17h
Time
C
Top 15 of GO Enrichment
pvalue
4e-07
3e-07
2e-07
1e-07
GO:0009607 response to biotic stimulus
GO:0043207 response to external biotic stimulus
GO:0051707 response to other organism
GO:0098542 defense response to other organism
GO:0044419 biological process involved in interspecies interaction between organisms
GO:0002376 immune system process
GO:0006952 defense response
GO:0006955 immune response
GO:0045087 innate immune response
GO:0009605 response to external stimulus
GO:0032787 monocarboxylic acid metabolic process
GO:0006950 response to stress
GO:0006631 fatty acid metabolic process
GO:0009056 catabolic process
GO:0072329 monocarboxylic acid catabolic process
GOterm
Gene Percent(%)
D
UPR^ER target
UP by HK-OP50
51
11
1306
E
Bthu
PA
Saur
HK-OP50
Smar
F
Phsp-4::GFP
HK-OP50
OP50
Phsp-4::GFP Fluorescence (relative intensity)
****
30
31
G
Pirg-5::GFP
HK-OP50
OP50
Pirg-5::GFP Fluorescence (relative intensity)
***
21
23

Figure 2

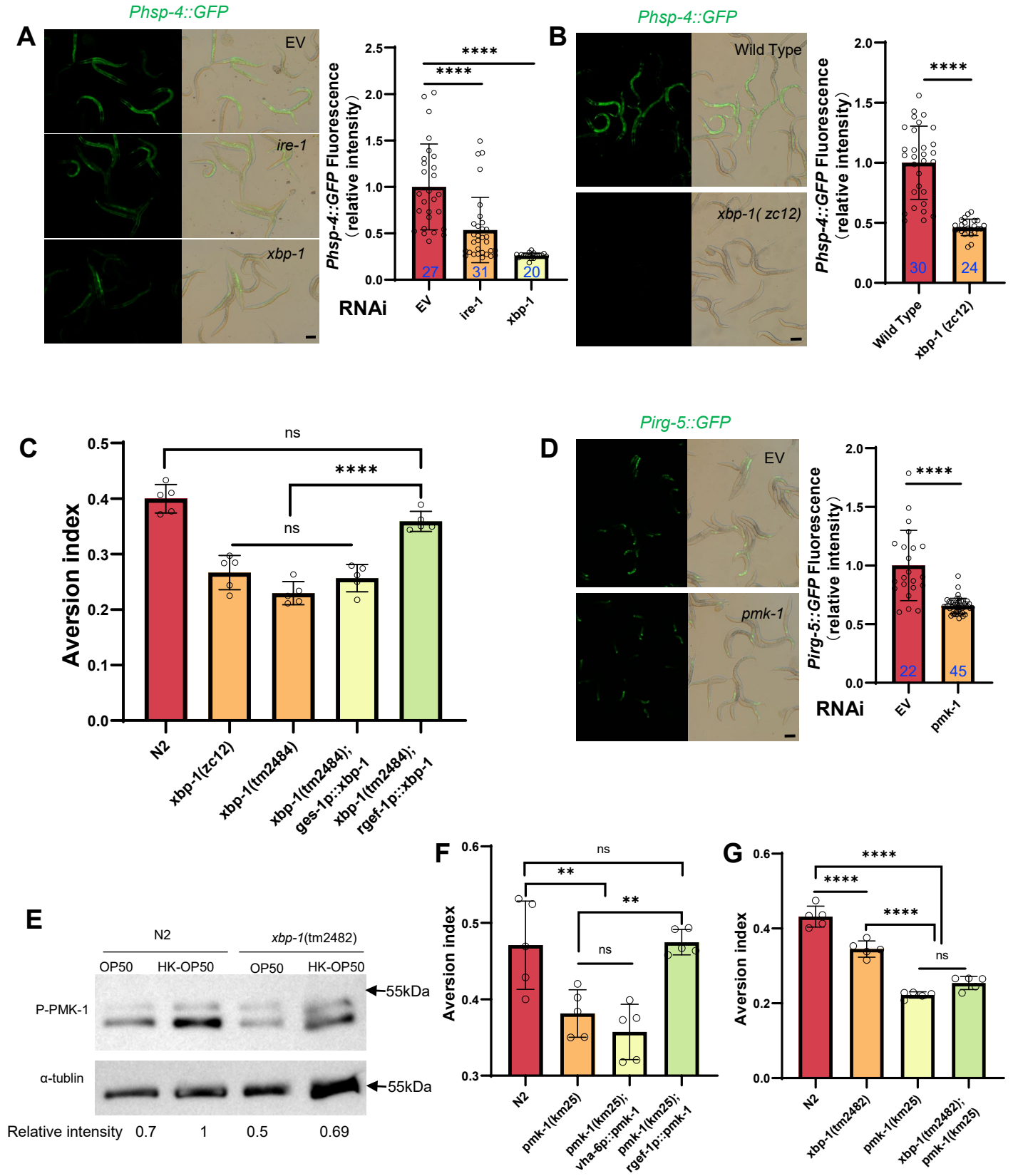
A
Phsp-4::GFP
EV
ire-1
xbp-1
Phsp-4::GFP Fluorescence (relative intensity)
****
****
27
31
20
RNAi
EV
ire-1
xbp-1
B
Phsp-4::GFP
Wild Type
xbp-1(zc12)
Phsp-4::GFP Fluorescence (relative intensity)
****
30
24
Wild Type
xbp-1 (zc12)
C
Aversion index
ns
****
ns
N2
xbp-1(zc12)
xbp-1(tm2484)
xbp-1(tm2484); ges-1p::xbp-1
xbp-1(tm2484); rgef-1p::xbp-1
D
Pirg-5::GFP
EV
pmk-1
Pirg-5::GFP Fluorescence (relative intensity)
****
22
45
RNAi
EV
pmk-1
E
N2
xbp-1(tm2482)
OP50
HK-OP50
OP50
HK-OP50
P-PMK-1
55kDa
α-tublin
55kDa
Relative intensity 0.7 1 0.5 0.69
F
Aversion index
ns
**
**
ns
N2
pmk-1(km25)
pmk-1(km25); vha-6p::pmk-1
pmk-1(km25); rgef-1p::pmk-1
G
Aversion index
****
****
****
ns
N2
xbp-1(tm2482)
pmk-1(km25)
xbp-1(tm2482); pmk-1(km25)

Figure 3

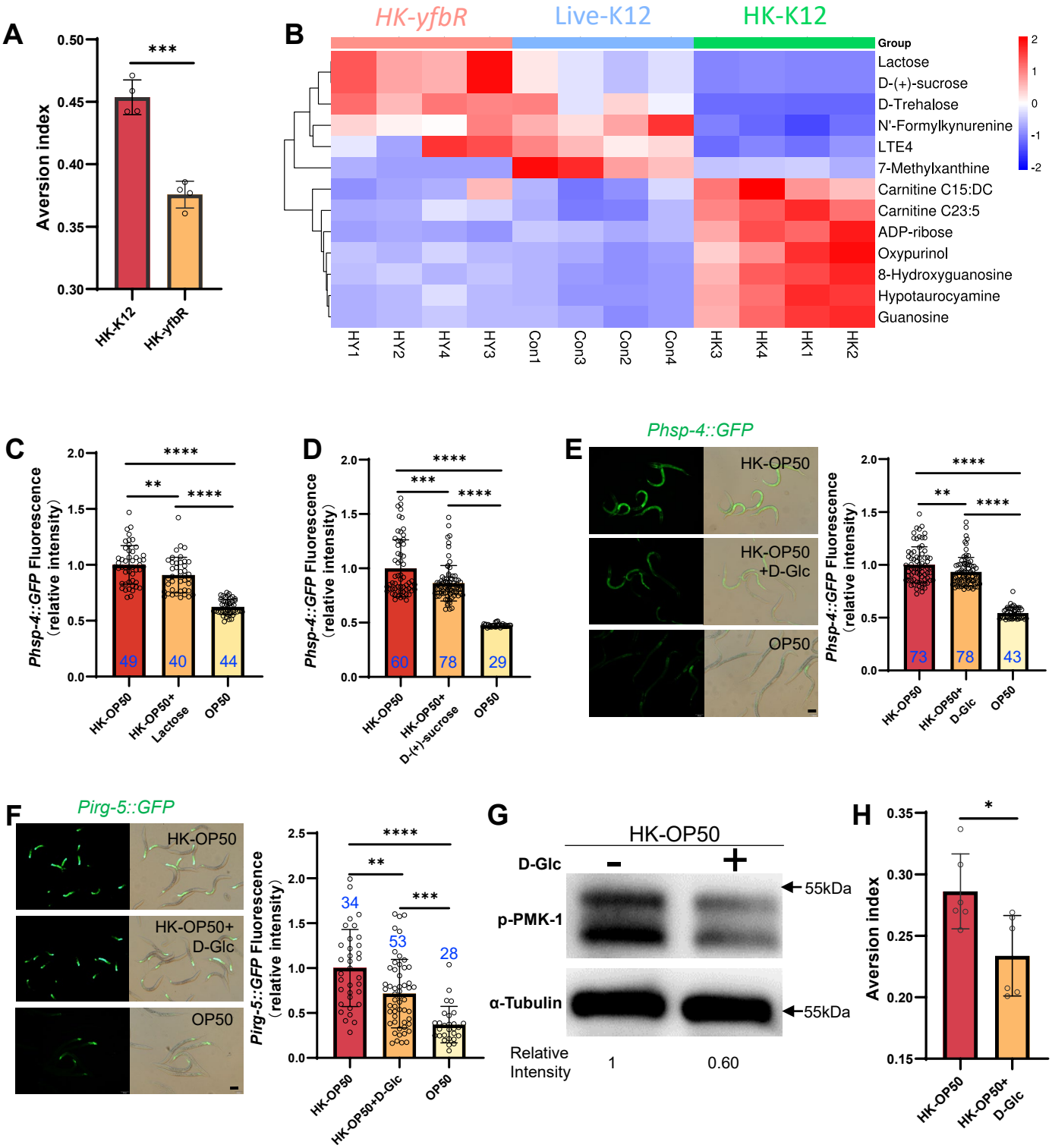
A
Aversion index
0.50
0.45
0.40
0.35
0.30
***
HK-K12
HK-yfbR
B
HK-yfbR
Live-K12
HK-K12
Group
Lactose
D-(+)-sucrose
D-Trehalose
N'-Formylkynurenine
LTE4
7-Methylxanthine
Carnitine C15:DC
Carnitine C23:5
ADP-ribose
Oxypurinol
8-Hydroxyguanosine
Hypotaurocyamine
Guanosine
HY1
HY2
HY4
HY3
Con1
Con3
Con2
Con4
HK3
HK4
HK1
HK2
2
1
0
-1
-2
C
Phsp-4::GFP Fluorescence (relative intensity)
2.0
1.5
1.0
0.5
0.0
****
**
****
49
40
44
HK-OP50
HK-OP50+ Lactose
OP50
D
Phsp-4::GFP Fluorescence (relative intensity)
****
***
****
60
78
29
HK-OP50
HK-OP50+ D-(+)-sucrose
OP50
E
Phsp-4::GFP
HK-OP50
HK-OP50 +D-Glc
OP50
Phsp-4::GFP Fluorescence (relative intensity)
****
**
****
73
78
43
HK-OP50
HK-OP50+ D-Glc
OP50
F
Pirg-5::GFP
HK-OP50
HK-OP50+ D-Glc
OP50
Pirg-5::GFP Fluorescence (relative intensity)
2.5
2.0
1.5
1.0
0.5
0.0
****
**
***
34
53
28
HK-OP50
HK-OP50+D-Glc
OP50
G
HK-OP50
D-Glc
-
+
p-PMK-1
α-Tubulin
55kDa
55kDa
Relative Intensity
1
0.60
H
Aversion index
0.35
0.30
0.25
0.20
0.15
*
HK-OP50
HK-OP50+ D-Glc

Figure 4

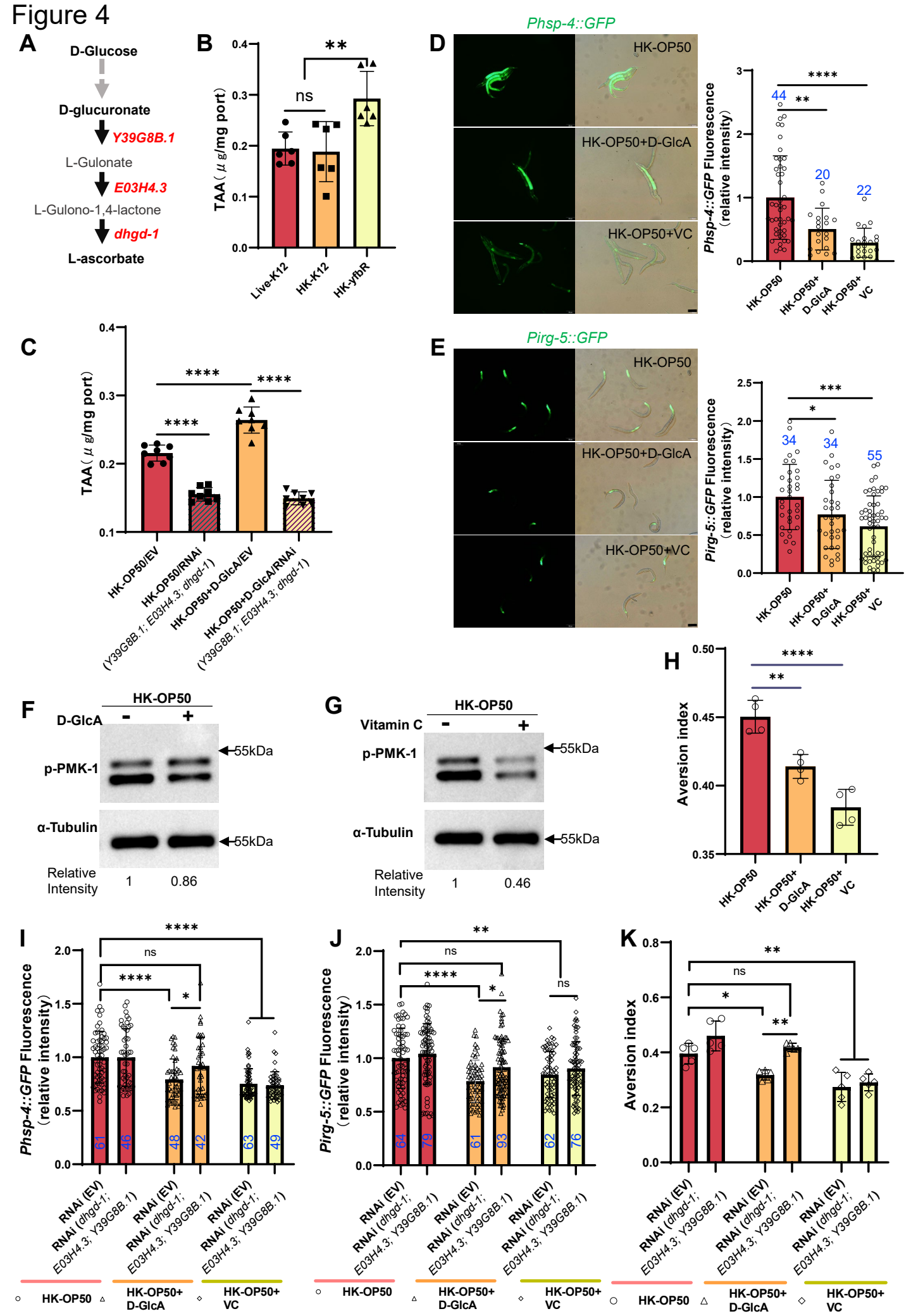
A
D-Glucose
D-glucuronate
Y39G8B.1
L-Gulonate
E03H4.3
L-Gulono-1,4-lactone
dhgd-1
L-ascorbate
B
TAA（μg/mg port）
ns
**
Live-K12
HK-K12
HK-yfbR
C
TAA（μg/mg port）
****
****
****
HK-OP50/EV
HK-OP50/RNAi (Y39G8B.1; E03H4.3; dhgd-1)
HK-OP50+D-GlcA/EV
HK-OP50+D-GlcA/RNAi (Y39G8B.1; E03H4.3; dhgd-1)
D
Phsp-4::GFP
HK-OP50
HK-OP50+D-GlcA
HK-OP50+VC
Phsp-4::GFP Fluorescence (relative intensity)
****
**
44
20
22
HK-OP50
HK-OP50+ D-GlcA
HK-OP50+ VC
E
Pirg-5::GFP
HK-OP50
HK-OP50+D-GlcA
HK-OP50+VC
Pirg-5::GFP Fluorescence (relative intensity)
***
*
34
34
55
HK-OP50
HK-OP50+ D-GlcA
HK-OP50+ VC
F
HK-OP50
D-GlcA
-
+
p-PMK-1
α-Tubulin
55kDa
55kDa
Relative Intensity
1
0.86
G
HK-OP50
Vitamin C
-
+
p-PMK-1
α-Tubulin
55kDa
55kDa
Relative Intensity
1
0.46
H
Aversion index
****
**
HK-OP50
HK-OP50+ D-GlcA
HK-OP50+ VC
I
Phsp-4::GFP Fluorescence (relative intensity)
****
ns
****
*
61
46
48
42
63
49
RNAi (EV)
RNAi (dhgd-1; E03H4.3; Y39G8B.1)
HK-OP50
HK-OP50+ D-GlcA
HK-OP50+ VC
J
Pirg-5::GFP Fluorescence (relative intensity)
**
ns
****
*
ns
64
79
61
93
62
76
RNAi (EV)
RNAi (dhgd-1; E03H4.3; Y39G8B.1)
HK-OP50
HK-OP50+ D-GlcA
HK-OP50+ VC
K
Aversion index
**
ns
*
**
RNAi (EV)
RNAi (dhgd-1; E03H4.3; Y39G8B.1)
HK-OP50
HK-OP50+ D-GlcA
HK-OP50+ VC

Figure 5

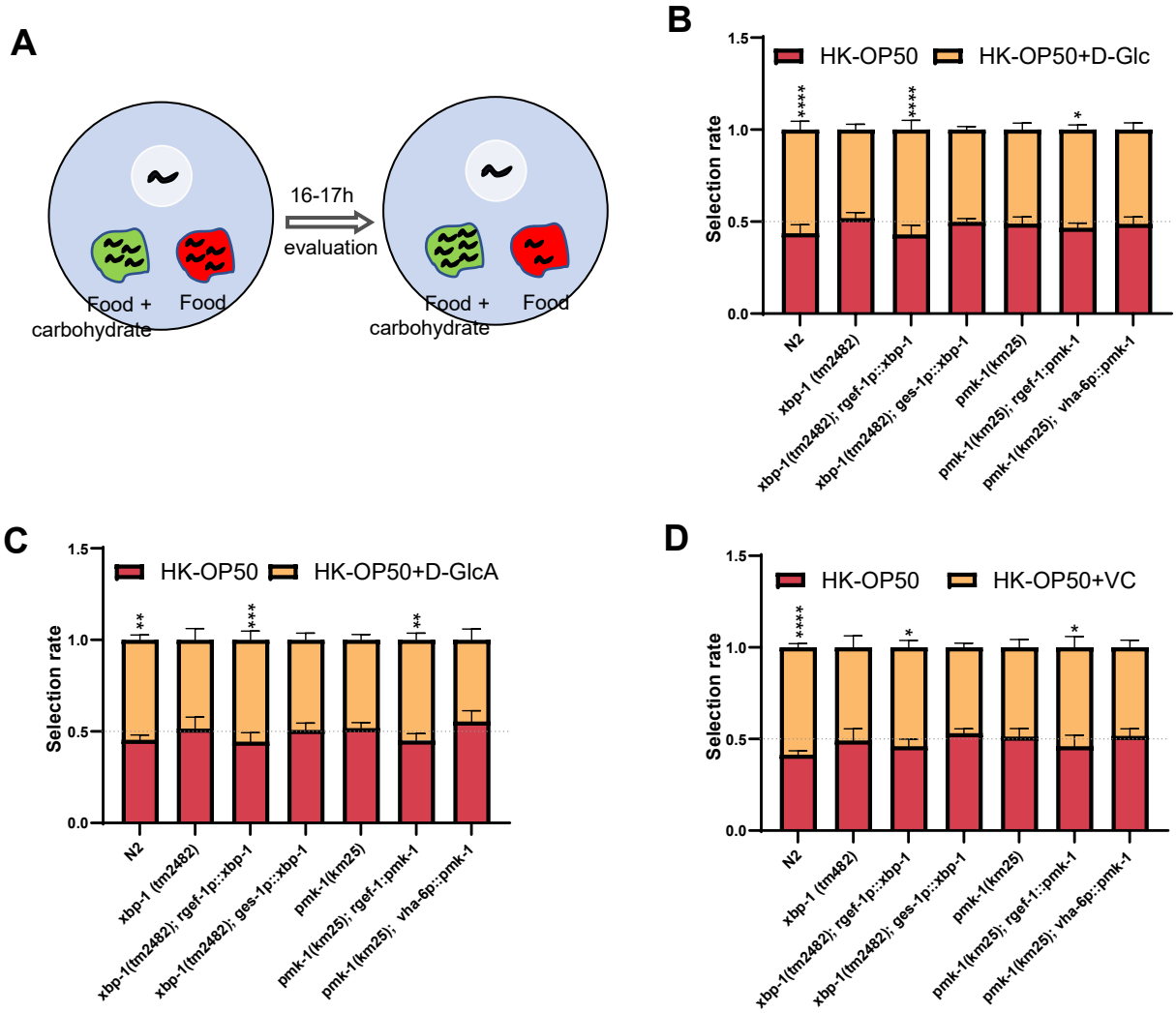
A
16-17h
evaluation
Food +
carbohydrate
Food
Food +
carbohydrate
Food
B
HK-OP50
HK-OP50+D-Glc
Selection rate
1.5
1.0
0.5
0.0
****
****
*
N2
xbp-1 (tm2482)
xbp-1(tm2482); rgef-1p::xbp-1
xbp-1(tm2482); ges-1p::xbp-1
pmk-1(km25)
pmk-1(km25); rgef-1:pmk-1
pmk-1(km25); vha-6p::pmk-1
C
HK-OP50
HK-OP50+D-GlcA
Selection rate
1.5
1.0
0.5
0.0
**
***
**
N2
xbp-1 (tm2482)
xbp-1(tm2482); rgef-1p::xbp-1
xbp-1(tm2482); ges-1p::xbp-1
pmk-1(km25)
pmk-1(km25); rgef-1:pmk-1
pmk-1(km25); vha-6p::pmk-1
D
HK-OP50
HK-OP50+VC
Selection rate
1.5
1.0
0.5
0.0
****
*
*
N2
xbp-1 (tm482)
xbp-1(tm2482); rgef-1p::xbp-1
xbp-1(tm2482); ges-1p::xbp-1
pmk-1(km25)
pmk-1(km25); rgef-1::pmk-1
pmk-1(km25); vha-6p::pmk-1

Figure 6

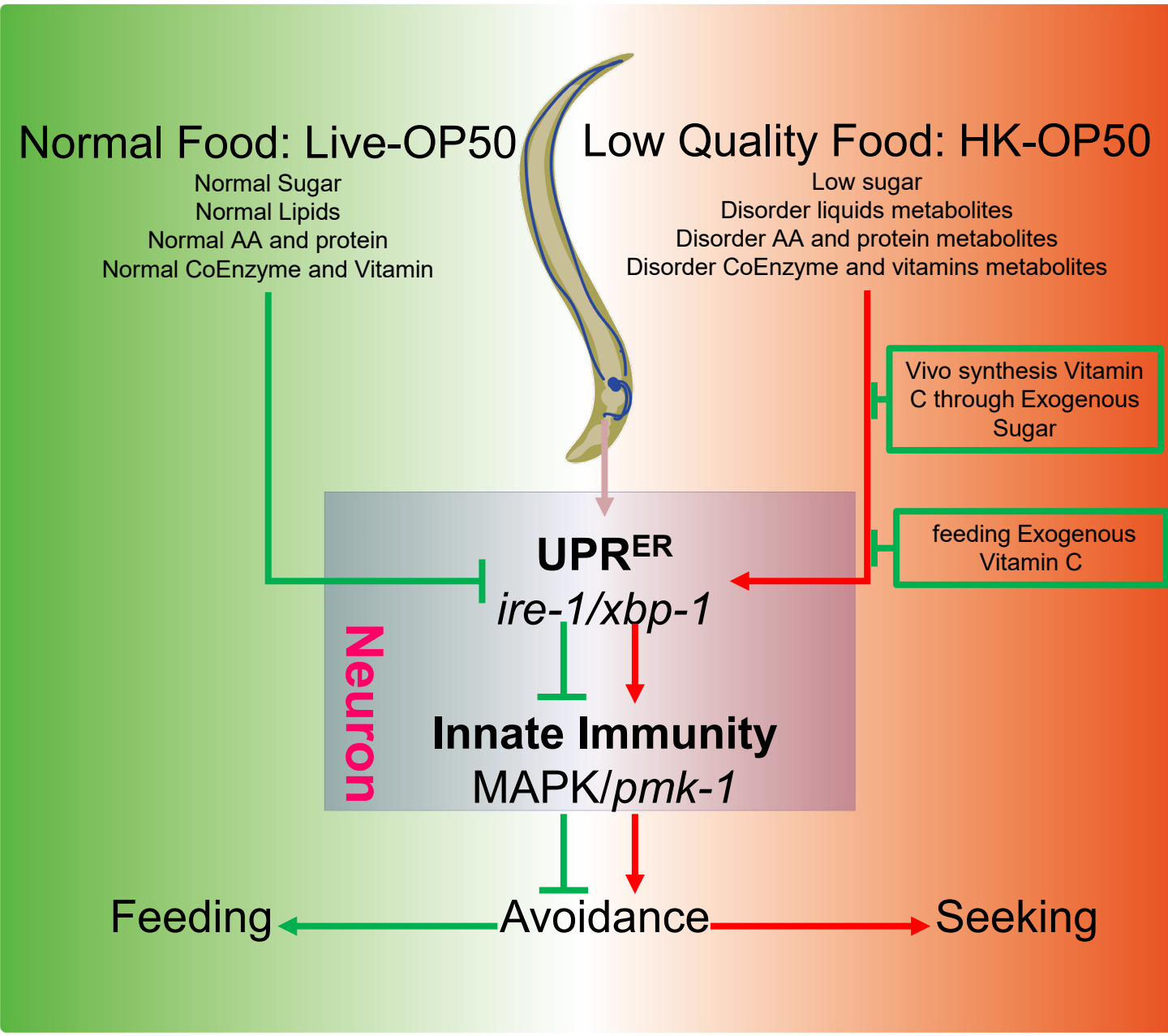
Normal Food: Live-OP50
Normal Sugar
Normal Lipids
Normal AA and protein
Normal CoEnzyme and Vitamin
Low Quality Food: HK-OP50
Low sugar
Disorder liquids metabolites
Disorder AA and protein metabolites
Disorder CoEnzyme and vitamins metabolites
Vivo synthesis Vitamin C through Exogenous Sugar
feeding Exogenous Vitamin C
UPR^ER
ire-1/xbp-1
Neuron
Innate Immunity
MAPK/pmk-1
Feeding
Avoidance
Seeking